NOTE I

I. INTRODUCTION - A Sketch on Early History of Response Spectrum

The first practical steps, which initiated the engineering work on the design of earthquake resistant structures, accompanied the introduction of the *seismic coefficient* (*shindo* in Japan, and *rapporto sismico* in Italy, for example), and started to appear following the destructive earthquakes in San Francisco, California, in 1906, Messina-Reggio, Italy, in 1908 , and Tokyo, Japan, in 1923. The first seismic design code was introduced in Japan in 1924 following the 1923 earthquake. In California the work on the code development started in 1920s, but it was not after the Long Beach earthquake in 1933 that the Field Act was finally adopted in 1934 .

In early 1900s, at most universities, engineering curricula did not include advanced mathematics and mechanics, both essential for teaching analysis of the dynamic response of structures. This lack in theoretical preparation is reflected in the view of C. Derleth, civil engineering professor and Dean of Engineering at U.C. Berkeley, who commented after the 1906 earthquake:

Many engineers with whom the writer has talked appear to have the idea that earthquake stresses in framed structures can be calculated, so that rational design to resist earthquake destruction can be made, just as one may allow for dead and live loads, or wind and impact stresses. Such calculations lead to no practical conclusions of value (Derleth 1907).

A comment by A. Ruge (1940), the first professor of engineering seismology at Massachusetts Institute of Technology, that "the natural tendency of average design engineer is to throw up his hands at the thought of making any dynamical analysis at all..", made three decades later, shows that the progress was slow.

In 1929, at University of Michigan, in Ann Arbor, first lectures were organized in the Summer School of Mechanics, by S. Timoshenko (1878-1972), with participation of A. Nádai, R. V. Southwell and H. M. Westergaard. "After the first session of the summer school in 1929, the number of doctoral students in mechanics….started rapidly to increase" (Timoshenko 1968). In the summer of 1933, M.A. Biot was among the young post-doctoral students, who took part in Timoshenko's summer school (Mindlin 1989, Bolley 2005).

In southern California, studies of earthquakes, and the research in theoretical mechanics, were expanded by R.Millikan, who became the first president of Caltech, in 1921. Millikan completed his Ph.D. studies in Physics, at Columbia University, in 1895, and following recommendation of his advisor M. Pupin spent a year in Germany. This visit to Europe appears to have influenced many of Millikan's later decisions while recruiting the leading Caltech faculty two decades later. In 1921 H.O. Wood invited Millikan to serve on the Advisory Committee in Seismology. The work on that committee and Millikan's

interest in earthquakes were also significant for several subsequent events. In 1926 C. Richter, and in 1930 B. Gutenberg joined the seismological laboratory. In the area of applied mechanics, Millikan invited Theodor von Karman, and in 1930 von Karman became the first director of the Guggenheim Aeronautical Laboratory. It was Millikan's vision and his ability to anticipate future developments, which brought so many leading minds to a common place of work, creating environment, which made the first theoretical formulation of the concept of the response spectrum method possible.

This year, 2007, marks the 75-th anniversary of the formulation of the concept of the Response Spectrum Method (RSM) in 1932. Since 1932 the RSM evolved into the essential tool and the central theoretical framework, in short a conditio sine qua non, for Earthquake Engineering. The mathematical formulation of the RSM first appeared in the doctoral dissertation of M.A. Biot (1905-1985) in 1932, and in two of his papers (Biot 1933; 1934). Biot defended his Ph.D. thesis at Caltech, in June of 1932, and presented a lecture on the method to the Seismological Society of America meeting, which was held at Caltech, in Pasadena, also in June of 1932. Theodore von Karman, Biot's advisor, played the key role in guiding his student, and in promoting his accomplishments. After the method of solution was formulated, Biot and von Karman searched for an optimal design strategy. A debate at the time was whether a building should be designed with a soft first floor, or it should be stiff throughout its height, to better resist earthquake forces. An excerpt from New York Herald Tribune, in June of 1932, illustrates this:

Shock Proof Buildings Sought by Scientists.
Rigid or Flexible Materials, Their Difference in Theory

A building proof against earthquakes is the goal of Dr. Theodor von Karman and Dr. M. Biot, of California Institute of technology. Dr. von Karman described to the American Society of Mechanical Engineers, whose convention was held recently at Yale, studies of the amount of shock, which various types of buildings have undergone in Japan, South America and California. Their researches are being conducted at the Institute's Guggenheim Aeronautical Laboratory.

One of the principal problems is to decide whether a rigid or flexible structure is better. Some scientists contend the first is preferable; others would make the ground floor of tall buildings flexible.

Pointing out that the reinforced concrete is superior to steel in absorbing the shocks, Dr. von Karman's personal belief is that the building should be constructed to shake "with the rhythm of the earth's movements."

Biot's interest in the maxima of the transient response in solids and in fluids preceded, and extended beyond earthquake engineering. After he formulated the concept of the RSM, he extended it to other vibrational problems, as in analysis of aircraft landing gear, for example. Biot briefly returned to the subject of earthquake engineering almost ten years later, presenting response spectral amplitudes of several earthquakes, which he calculated using the torsional pendulum at Columbia University (Biot 1941). In 1942 he presented a review of response spectrum method, discussed the effects of flexible soil on the rocking period of a rigid block (Biot 2006), and described the spectrum superposition method based on the sum of absolute modal maxima (Biot 1942). After 1942 Biot moved on to other subjects, making fundamental contributions to many other fields. He did not

write papers on earthquake engineering (Trifunac 2005), but followed closely and with interest the work of others. A complete list of Biot's publications can be found in

Theodor von Karman (left) and Maurice A. Biot (right) at professor von Karman's house in Pasadena (circa 1932)

Trifunac (2006), and of his patents and awards, in the introduction to Vol.14 of the Journal of Mathematical and Physical Sciences, published in Madras, India, in 1980, on the occasion of his seventieth birthday anniversary.

The RSM remained in the academic sphere of research for almost 40 years, gaining engineering acceptance during the early 1970s. There were two main reasons for this. First, the computation of response to earthquake ground motion led to "certain rather formidable difficulties" (Housner, 1947), and, second, there were only a few well-recorded accelerograms that could be used for response studies. This started to change in 1960s with arrival of digital computers and with commercial availability of strong-motion accelerographs. Before the digital computer age, the computation of response was time consuming, and the results were unreliable (Trifunac 2003). By the late 1960s and early 1970s, the digitization of analog accelerograph records and the digital computation of ground motion and of the response spectra were developed completely and tested for accuracy. Then, in 1971, with the occurrence of the San Fernando, California, earthquake, the modern era of RSM was launched. This earthquake was recorded by 241

accelerographs. By combining the data from the San Fernando earthquake with all previous strong-motion records, it become possible to launch the first comprehensive empirical scaling analyses of response spectral amplitudes (Lee 2002; 2007).

References

Biot, M.A. (1932). "Vibrations of Buildings During Earthquakes," Chapter II in Ph.D. Thesis No. 259, entitled "Transient Oscillations in Elastic System," Aeronautics Department, Calif. Inst. of Tech., Pasadena, California.

Biot, M.S. (1933). "Theory of Elastic Systems Vibrating Under Transient Impulse With an Application to Earthquake-Proof Buildings," *Proc. National Academy of Sciences*, 19(2), pp. 262–268.

Biot, M.A. (1934). "Theory of Vibration of Buildings During Earthquakes," *Zeitschrift für. Angewandte Matematik und Mechanik*, 14(4), pp. 213–223.

Biot, M.A. (1941). "A Mechanical Analyzer for the Prediction of Earthquake Stresses," *Bull. Seism. Soc. Amer*., 31, pp. 151–171.

Biot, M.A. (1942). "Analytical and Experimental Methods in Engineering Seismology," *ASCE Transactions*, 108, pp. 365–408.

Biot, M.A. (2006). Influence of Foundation on Motion of Blocks, *Soil Dynamics and Earthquake Engineering,* 26(6-7), pp.486-490.

Boley, B.A. (2005). Maurice Biot – He is one of us, *Proc. Biot centennial conference,* Norman, Oklahoma, in *Poromechanics III,* Edited by Abousleiman, Y.N., Cheng, A.H., and Ulm, F.J., pp. 7-9.

Derleth, C. (1907). The Effects of the San Francisco Earthquake of April 18-th, 1906 on Engineering Constructions, *Transactions of the American Society of Civil Engineers,* Vol. LIX, December.

Housner, G.W. (1947). "Characteristics of Strong Motion Earthquakes," *Bull. Seism. Soc. Amer*., Vol. 37, No.1, pp. 19–31.

Lee, V.W. (2002). "Empirical Scaling of Strong Earthquake Ground Motion-Part I: Attenuation and Scaling of Response Spectra," *Indian Society of Earthquake Technology Journal*, Vol.39, No.4, pp. 219–254.

Lee, V.W. (2007). Empirical Scaling and Regression Methods for Earthquake Strong-Motion Response Spectra – A Review, *Indian Society of Earthquake Technology journal*, **44**(1), (in press).

Mindlin, R.D. (1989) Maurice Anthony Biot, in Memorial Tributes: Natl. Academy of Engineering, Vol. 3, pp. 31–35.

Ruge, A. (1940). Ruge on Earthquakes and Structures, *Transactions of the American Society of Civil Engineers,* Vol.105.

Timoshenko, S.P. (1968). As I Remember, Van Nostrand Co., Princeton.

Trifunac, M.D. (2003) 70th Anniversary of Biot Spectrum, 23rd Annual ISET Lecture, *Indian Society of Earthquake Technology Journal,* Paper 431, Vol. 40, No. 1, pp. 19–50.

Trifunac, M.D. (2005). Scientific citations of M. A. Biot, *Proc. Biot centennial conference,* Norman, Oklahoma, in *Poromechanics III,* Edited by Abousleiman, Y.N., Cheng, A.H., and Ulm, F.J., pp. 11-17.

Trifunac, M.D. (2006). Biographical Sketch and Publications of M. A. Biot, *Soil Dynamics and Earthquake Engineering,* 26(6-7), pp. 718-724.

Von Karman, T. and Edson, L. (1967). The Wind and Beyond, Little, Brown and Co., Boston.

.

NOTE A

A. RESPONSE SPECTRA - An Outline of the Method

Single -degree- of -freedom system.

A single-degree-of-freedom system corresponding to a one-story structure is schematically shown in figure A.1. For vibration z(t) of its base, the differential equation of linear motion is

$$m\ddot{x} + c\dot{x} + kx = -m\ddot{z}\ , \tag{A.1}$$

where x is the relative displacement between the structure and its base and $-m\ddot{z}$ represents the inertial force applied to the mass m, supported on two columns, which has the equivalent spring constant k. Energy dissipation is assumed to be of viscous nature, with damping force proportional to the relative velocity between the mass and its foundation, and c being the damping constant.

The natural frequency ω_n and the fraction of critical damping ζ are defined as

$$\omega_n^2 = \frac{k}{m} \tag{A.2}$$

and

$$\varsigma = \frac{c}{2\sqrt{km}}\ . \tag{A.3}$$

Equation (A.1) then becomes

$$\ddot{x} + 2\omega_n\varsigma\dot{x} + \omega_n^2 x = -\ddot{z}\ . \tag{A.4}$$

For any general motion of the support z(t), the relative displacement x(t) can be computed from the Duhamel integral (Biot, 1932; 1933; 1934; von Karman and Biot, 1940) . For zero initial conditions, the expression for x(t) takes the form

$$x(t) = \frac{-1}{\omega_n\sqrt{1-\varsigma^2}}\int_0^t \ddot{z}(\tau)e^{-\varsigma\omega_n(t-\tau)}\sin\omega_n\sqrt{1-\varsigma^2}\,(t-\tau)d\tau. \tag{A.5}$$

Thus, the linear relative response of the structure is characterized by its natural period $T_n = \frac{2\pi}{\omega_n}$, the fraction of critical damping ζ, and the nature of the base acceleration, $\ddot{z}(\tau)$.

The relative displacement x(t) is important for earthquake-resistant design because the strains in the structure are directly proportional to the relative displacements. The total shear force V_B (Figure A.1), for example, exerted by the columns on the ground is

$$V_B(t) = kx(t). \tag{A.6}$$

The exact relative velocity $\dot{x}(t)$ follows directly from (A.5):

$$\dot{x}(t) = -\int_0^t \ddot{z}(\tau) e^{-\varsigma\omega_n(t-\tau)} \cos\omega_n\sqrt{1-\varsigma^2}\,(t-\tau)d\tau$$

$$+\frac{\varsigma}{\sqrt{1-\varsigma^2}}\int_0^t \ddot{z}(\tau) e^{-\varsigma\omega_n(t-\tau)} \sin\omega_n\sqrt{1-\varsigma^2}\,(t-\tau)d\tau\,. \tag{A.7}$$

The absolute acceleration $\ddot{y}(t)$ of the mass m is obtained by further differentiation of $\dot{x}(t)$, noting that $\ddot{y}(t) = \ddot{x}(t) + \ddot{z}(t)$. It is:

$$\ddot{y}(t) = \omega_n \frac{\left(1-2\varsigma^2\right)}{\sqrt{1-\varsigma^2}}\int_0^t \ddot{z}(\tau) e^{-\varsigma\omega_n(t-\tau)} \sin\omega_n\sqrt{1-\varsigma^2}\,(t-\tau)d\tau$$

$$+\frac{\varsigma}{\sqrt{1-\varsigma^2}}\int_0^t \ddot{z}(\tau) e^{-\varsigma\omega_n(t-\tau)} \cos\omega_n\sqrt{1-\varsigma^2}\,(t-\tau)d\tau. \tag{A.8}$$

The absolute acceleration $\ddot{y}$ is important for experimental measurements, because it is the quantity, which is the most simple to measure during strong, earthquake-induced vibrations. That is, an accelerograph located at that point records a close approximation to $\ddot{y}(t)$. The absolute acceleration also defines the seismic force on the mass m (figure A.1).

It may be concluded that of primary interest, for engineering applications, are the maximum absolute values of x(t), $\dot{x}(t)$, and $\ddot{y}(t)$ experienced during the earthquake response. These quantities are commonly defined as:

$$SD \equiv |x(t)|_{max} \tag{A.9}$$
$$SV \equiv |\dot{x}(t)|_{max} \tag{A.10}$$
$$SA \equiv |\ \ddot{y}(t)|_{max}\,. \tag{A.11}$$

SINGLE - DEGREE - OF - FREEDOM SYSTEM

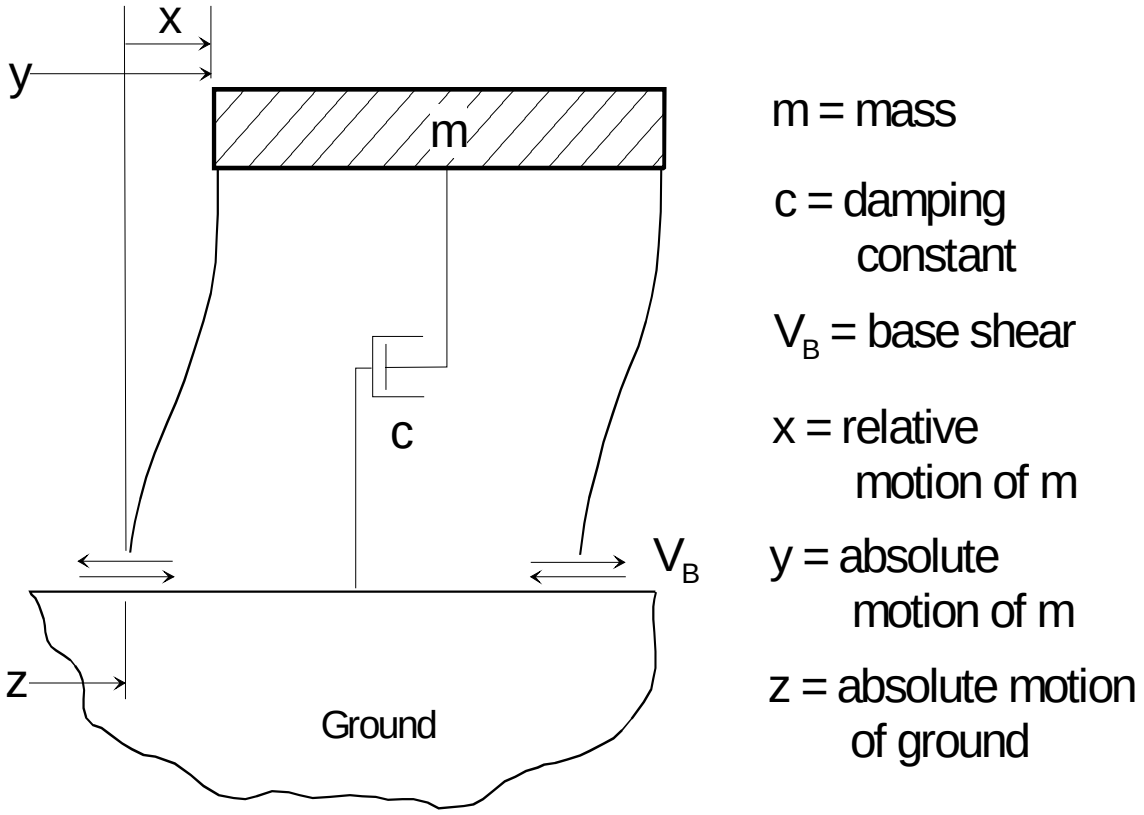

Fig. A.1 Single-degree-of-freedom system.

Plots of SD, SV, and SA versus the undamped natural period of vibration $T_n = \frac{2\pi}{\omega_n}$, for various fractions of critical damping ς, are called earthquake response spectra.

In typical engineering structures, the fraction of critical damping ζ is small. It is approximately 2% - 8% for buildings and 5% –10% for soil structures. Therefore, $\sqrt{1-\varsigma^2} \approx 1$ and the terms of order ζ and ζ^2 in equations (A.7) and (A.8) may be neglected. Furthermore, if the cosine term is replaced by a sine term in Equation (A.7) the following approximate relationships exist between the spectral quantities defined in (A.9), (A.10), and (A.11):

$$SD \approx \frac{T}{2\pi} SV \tag{A.12}$$

and

$$SA \approx \frac{2\pi}{T} SV. \tag{A.13}$$

For earthquake-like excitations, these approximations can be made plausible (Hudson, 1962). For engineering applications, it is convenient to use the following approximations

$$PSV = \frac{2\pi}{T} SD \tag{A.14}$$

and

$$PSA = \left(\frac{2\pi}{T}\right)^2 SD \tag{A.15}$$

because SD, PSV, and PSA can be conveniently plotted on the common tripartite logarithmic plot versus period. In the engineering literature, PSV and PSA are frequently referred to as "pseudo velocity" and "pseudo absolute acceleration."

Fourier Spectra and Response Spectra.

The Fourier spectrum of an input acceleration shows the significant frequency characteristics of recorded motion. For an accelerogram differing from zero in the time interval $0 < t < T$ the Fourier spectrum is defined as:

$$F(\omega) = \int_0^T \ddot{z}(\tau) e^{-i\omega\tau} d\tau \tag{A.16}$$

The Fourier amplitude spectrum is then given by the square root of the sum of the squares of the real and imaginary parts of F(ω)

$$FS \equiv | F(\omega) | = \left\{ \left[\int_0^T \ddot{z}(\tau) \cos\omega\tau d\tau \right]^2 + \left[\int_0^T \ddot{z}(\tau) \sin\omega\tau d\tau \right]^2 \right\}. \tag{A.17}$$

For an undamped oscillator there is a close relationship between the Fourier amplitude spectrum and the exact relative velocity response spectrum (Kawasumi, 1956; Rubin, 1961; Hudson, 1962). For ζ = 0, Equation (A.7) (dropping the subscript n on ω_n) reduces to:

$$\dot{x}(t) = -\int_0^t \ddot{z}(\tau) \cos\omega(t-\tau) d\tau. \tag{A.18a}$$

Expanding,

$$\dot{x}(t) = -\cos\omega\tau \int_0^t \ddot{z}(\tau) \cos\omega\tau d\tau + \int_0^t \ddot{z}(\tau) \sin\omega\tau d\tau. \tag{A.18b}$$

From definition (A.10) and from (A.18) it follows that:

$$SV = \left\{ \left[\int_0^{t_{max}} \ddot{z}(\tau) \cos\omega\tau d\tau \right]^2 + \left[\int_0^{t_{max}} \ddot{z}(\tau) \sin\omega\tau d\tau \right]^2 \right\}^{1/2}, \tag{A.19}$$

where $0 \le t_{max} \le T$ and t_{max} is the time at which the maximum response occurs.

Equations (A.17) and (A.19) show the similarity between the Fourier amplitude spectrum and the exact relative velocity spectrum. In the special case in which the time t_{max} coincides with the total duration of the earthquake T, the two spectra SV and FS become identical. In general, for $0 \le t_{max} \le T$, and $\zeta = 0$, SV is always greater than FS. In physical terms, FS is the maximum velocity of the undamped oscillator in the free vibration following the earthquake, whereas SV is the maximum velocity during both the earthquake and the subsequent free vibrations.

The Fourier amplitude spectrum FS is the quantity used in investigations of the earthquake mechanism as it relates to the amplitudes of recorded waves (Trifunac, 1993; 1995a,b). Similarly, the relative velocity spectrum SV characterizes the earthquake ground motion in terms of its influence on engineering structures. The above relation between SV and FS links the two measurements of the same physical phenomenon from different points of view.

Multi-Degree-of-Freedom Systems

An example of a fixed base multi-degree-of freedom system used to study vibrations of tall buildings is shown in figure A.2. In this model, masses m_i are lumped at the floor levels and are interconnected with massless columns, which have the equivalent spring constants k_i. Dashpots characterized by the damping constants c_i model the energy dissipation in this system. The shear force at each floor level is designated by V_i. V_n corresponds to the base shear acting between the structure and the rigid soil.

The system of equilibrium equations, one of which corresponds to each mass m_i, can be written in a compact matrix form as:

$$[m]\{\ddot{x}\} + [c]\{\dot{x}\} + [k]\{x\} = -\ddot{z}[m]\{I\}\,. \qquad \text{(A.20)}$$

Here, $[\cdot]$ designates a square n × n matrix, while $\{\cdot\}$ represents a column vector with n components. In general, the mass matrix [m], the damping matrix [c], and the stiffness matrix [k] may have all elements different from zero. For most structural models, however, like the one shown in figure A.2, these matrices have only the diagonal and few off-diagonal terms that differ from zero.

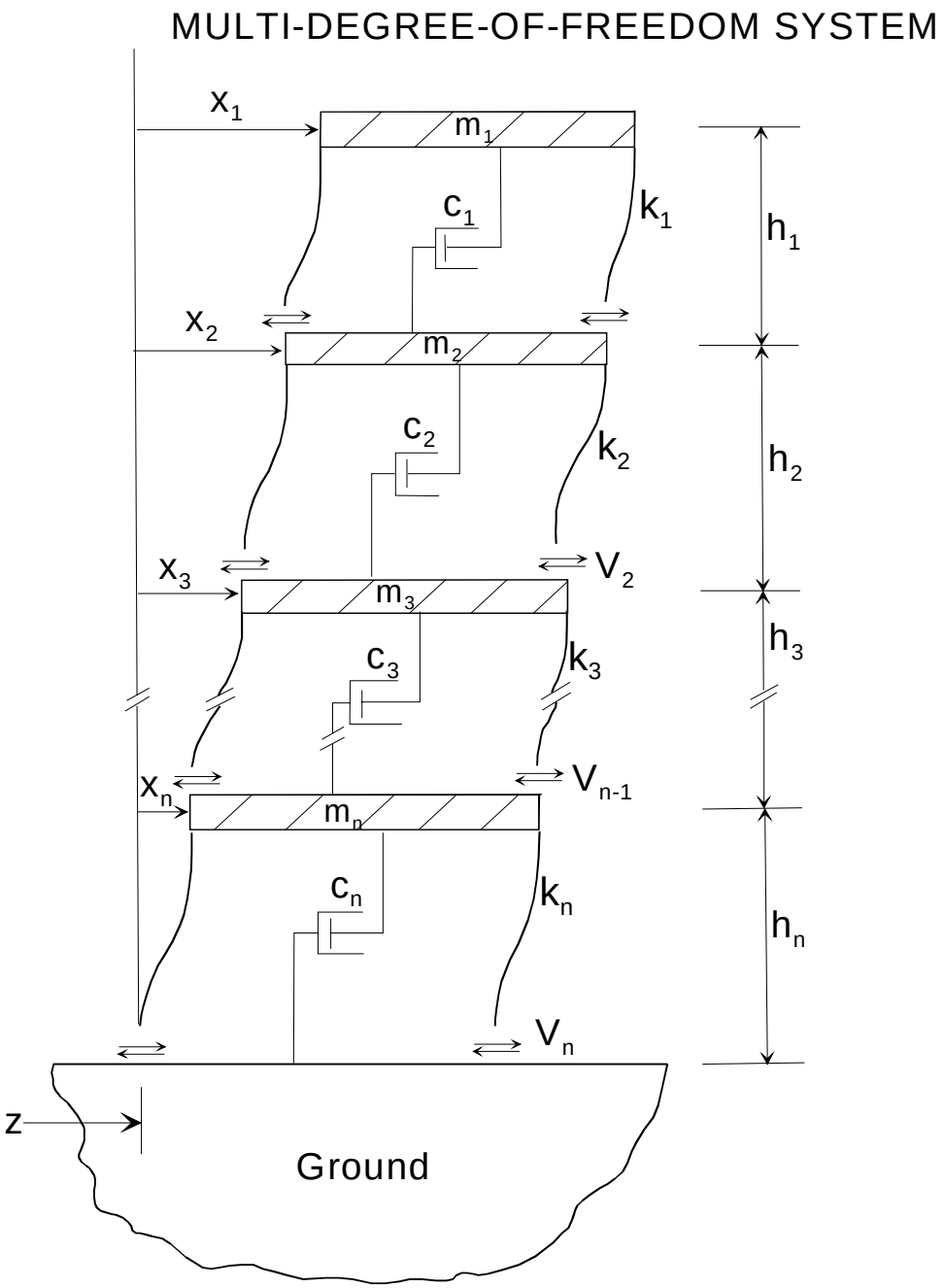

Fig. A.2 Multi-degree-of-freedom system.

In the special case in which the damping matrix [c] is a linear combination of the mass matrix and the stiffness matrix, a set of uncoupled coordinates $\{\xi\}$ and the corresponding transformation

$$\{x\} = [A]\ \{\xi\} \tag{A.21}$$

can be found in such a way that the classical normal mode solution is possible (Rayleigh, 1937; Caughey, 1959). Then, by substituting (A.21) into (A.20) and pre-multiplying (A.20) by the transpose of [A] there follows:

$$[A]^T[m][A]\{\ddot{\xi}\}+[A]^T[c][A]\{\dot{\xi}\}+[A]^T[k][A]\{\xi]=\ddot{z}[A]^T[m]\{I\}\,. \tag{A.22}$$

It is possible to normalize the coefficients of $\{\ddot{\xi}\}$ and $\{\xi\}$ in such a way that

$$[A]^T[m][A] = [I], \tag{A.23}$$

where [l] is the unit matrix, and

$$[A]^T[k][A] = [\omega^2]. \tag{A.24}$$

Denoting

$$[C] \equiv [A]^T[c]\ [A], \tag{A.25}$$

equation (A.22) becomes

$$[I]\{\ddot{\xi}\}+[C]\{\dot{\xi}\}+[\omega^2]\{\xi\}=-\ddot{z}[A]^T[m]\{I\}\,. \tag{A.26}$$

If [C] is a diagonal matrix,

$$[C]=\begin{bmatrix} 2\varsigma_1\omega_1 & 0 & 0 & \cdots & 0 \\ 0 & 2\varsigma_1\omega_1 & 0 & \cdots & \vdots \\ 0 & 0 & \ddots & & \vdots \\ \vdots & \vdots & & \ddots & \vdots \\ 0 & 0 & \cdots & \cdots & 2\varsigma_1\omega_1 \end{bmatrix}, \tag{A.27}$$

then equation (A.16) represents a set of n independent equations, each describing a single-degree-of-freedom system response in terms of a normal coordinate ξ_i :

$$\ddot{\xi}_i + 2\varsigma_i\omega_i\dot{\xi}_i + \omega_i^2\xi_i = -\ddot{z}\alpha_i\,, \tag{A.28}$$

where the constant

$$\alpha_i = \frac{\{A^i\}^T[m]\{I\}}{\{A^i\}^T[m]\{A^i\}};\quad i=1,2,3,...,n \tag{A.29}$$

is the mode participation factor. It shows the extent to which the i^{th} mode is excited by the earthquake.

As may be seen, the i[th] equation (A.28) is the same as Equation (A.5) for a single-degree-of-freedom oscillator. Its solution therefore becomes:

$$\xi_i(t) = \frac{-\alpha_i}{\omega_i\sqrt{1-\varsigma_i^2}} \int_0^t \ddot{z}(\tau) e^{-\varsigma_i\omega_i(t-\tau)} \sin \omega_i\sqrt{1-\varsigma_i^2}\,(t-\tau)\,d\tau. \qquad \text{(A.30)}$$

After solving (A.30) for all *i* the displacements, {x} can be calculated from

$$\{x(t)\} = [A]\ \{\xi(t)\}. \qquad \text{(A.31)}$$

When the displacements {x(t)} of masses are determined the earthquake forces $F_i(t)$ acting on each mass, m_i are given by

$$\{F(t)\} = [k]\ \{x(t)\}. \qquad \text{(A.32)}$$

The shear forces V_i (see fig. (A.2) are then:

$$\{V(t)\} = [S]\ \{x(t)\}, \qquad \text{(A.33)}$$

where [S] is the lower triangular matrix

$$[S] = \begin{bmatrix} 1 & 0 & 0 & \cdots & 0 \\ 1 & 1 & 0 & \cdots & 0 \\ 1 & 1 & 1 & & \vdots \\ \vdots & \vdots & \vdots & \ddots & \vdots \\ 1 & 1 & 1 & \cdots & 1 \end{bmatrix}. \qquad \text{(A.34)}$$

Similarly, the moments at each level of the structure (fig. A.2) are:

$$\{M(t)\}=[H][S][k]\{x(t)\}, \qquad \text{(A.35)}$$

where [H] is the lower triangular matrix

$$[H] = \begin{bmatrix} h_1 & 0 & 0 & \cdots & \cdots & 0 \\ h_1 & h_2 & 0 & \cdots & \cdots & 0 \\ h_1 & h_2 & h_3 & & & \vdots \\ \vdots & \vdots & \vdots & & \ddots & \vdots \\ h_1 & h_2 & h_3 & \cdots & h_{n-1} & h_n \\ & & & & & \end{bmatrix}. \qquad \text{(A.36)}$$

The ultimate objective of this analysis, from the engineering point of view, is to calculate the envelope of maximum response $\{x\}_{max}$, forces $\{F\}_{max}$,, shears $\{V\}_{max}$, and moments $\{M\}_{max}$, which are to be used for design purposes. Here, $\{\cdot\}_{max}$ defines the following operation:

$$\{g\}_{max} \equiv \begin{Bmatrix} g_{1_{max}} \\ g_{2_{max}} \\ \vdots \\ g_{n_{max}} \end{Bmatrix}. \qquad (A.37)$$

It may be noted that the maximum response vector, $\{x\}_{max}$, for example, does not define the response condition at any one time but the maximum response experienced by the different levels of a structure during the entire time history of the analysis.

Response Spectrum Superposition

In the preceding sections it was demonstrated that for multi-degrees-of-freedom, the dynamic response of the r-th mode alone may be described by the equation that corresponds to a single-degree-of-freedom system (see Equation's (A.4), and (A.28), and that the total displacement response may be computed by adding contributions of each individual mode (eq. (A.31)). For example, the contribution of the r-th mode to the total displacement of a multi-degree-of-freedom system would be:

$$\{x^{(r)}(t)\} = \frac{\{A^{(r)}\}\alpha_r}{\omega_i\sqrt{1-\varsigma_r^2}} \int_0^t \ddot{z}(\tau) e^{-\varsigma_r \omega_r (t-\tau)} \sin \omega_r \sqrt{1-\varsigma_r^2}\,(t-\tau) d\tau \ . \qquad (A.38)$$

This contribution is seen to be directly proportional to $1/\omega_r\sqrt{1-\varsigma_r^2}$ times the integral term and will depend on the integral's maximum absolute value. The latter was already defined in Equation (A.5) and its absolute value SD was given by Equation (A.9). Thus, in terms of displacement and velocity spectra (equations (A.9) through (A.15)) equation (A.38) can be written as

$$\{|\, x^{(r)}(t)\,|\}_{max} = \{|\, A^{(r)}\,|\}\alpha_r SD^{(r)} = \{|\, A^{(r)}\,|\}\alpha_r \frac{T_r}{2\pi} SV^{(r)}, \qquad (A.39)$$

where the superscripts (r) on SD and SV indicate that these spectral values are computed for damping ζ_r and frequency $\omega_r = \dfrac{2\pi}{T_r}$, corresponding to the r-th mode of vibration. However, the different modal maxima do not occur at the same time, and therefore the individual modes do not simultaneously contribute their peak values to the maximum total response.

The sum of maximum modal responses (Biot, 1942)

$$\sum_{r=1}^{n} \{|\, x^{(r)}(t)\,|\}_{\max} = [|\, A\,|] \begin{Bmatrix} SD^{(1)} \\ SD^{(2)} \\ \vdots \\ SD^{(n)} \end{Bmatrix} \tag{A.40}$$

would clearly give an upper bound to the total system response, but at the same time may be too conservative. An alternative approach, based on statistical considerations (Goodman, et al., 1958), is to take the square root of the sum of the squares of the individual modal maxima. This method (RMS) has been shown to give reasonable results (Jennings and Newmark, 1960) for structures in which the main contributions come from the lowest few modes. The question of mode superposition has been studied extensively (Amini and Trifunac, 1985; Gupta and Trifunac, 1987a,b,c; Merchant and Hudson, 1962), and the conditions under which a meaningful degree of conservatism can be achieved have been determined. When the maxima of each response quantity have been determined from equations analogous to equation (A.39), the RMS approximation is given by:

$$\{x\}_{\max} \approx \begin{Bmatrix} \left[\sum_{i=1}^{n} \left(x^i_{1_{\max}}\right)^2\right]^{1/2} \\ \left[\sum_{i=1}^{n} \left(x^i_{2_{\max}}\right)^2\right]^{1/2} \\ \vdots \\ \left[\sum_{i=1}^{n} \left(x^i_{n_{\max}}\right)^2\right]^{1/2} \end{Bmatrix} \tag{A.41}$$

Analogous expressions for $\{V\}_{\max}$ and $\{M\}_{\max}$ follow from equation (A.41).

The above-described response spectrum superposition method provides only an approximate indication of the maximum response in the multi-degree-of-freedom systems. The advantage of this method is that it avoids lengthy computations associated with the exact method and at the same time takes into account the dynamic nature of the problem. It can often provide reasonable results for design purposes.

.

NOTE B

B. Computation of Response Spectra

For the standard corrected accelerograms (Trifunac, et al, 1971), which are available at equally spaced time intervals Δt, an approach based on the exact analytical solution of the Duhamel integral for the successive linear segments of excitation appears to be the most practical. This approach is described in Nigam and Jennings (1968). The important features of this method are briefly summarized here.

The differential equation for the relative motion x(t) of a single-degree-of-freedom oscillator subjected to base acceleration a(t) is given by:

$$\ddot{x} + 2\omega\varsigma\dot{x} + \omega^2 x = -a(t) \tag{B.1}$$

where, ζ = fraction of critical damping and ω = the natural frequency of vibration of the oscillator. For a(t), given by a segmentally linear function for $t_i \le t \le t_{i+1}$, (B.1) becomes:

$$\ddot{x} + 2\omega\varsigma\dot{x} + \omega^2 x = -a_i + \frac{\Delta a_i}{\Delta t}(t - t_i)\,, \tag{B.2}$$

where

$$\Delta t = t_{i+1} - t_i = \text{const.} \tag{B.3}$$

and

$$\Delta a_i = a_{i+1} - a_i\,. \tag{B.4}$$

The solution of equation (B.2), for $t_i \le t \le t_{i+1}$, then becomes:

$$x(t) = e^{-\varsigma\omega(t-t_i)}\left[C_1 \sin\omega_d(t-t_i) + C_2\cos\omega_d(t-t_i)\right] - \frac{a_i}{\omega^2} + \frac{2\varsigma}{\omega^3}\frac{\Delta a_i}{\Delta t} - \frac{1}{\omega^2}\frac{\Delta a_i}{\Delta t}(t-t_i), \tag{B.5}$$

where

$$\omega_d \equiv \omega\sqrt{1-\varsigma^2}\,. \tag{B.5}$$

Setting $x = x_i$ and $\dot{x} = \dot{x}_i$ at $t = t_i$, C_1 and C_2 become:

$$C_1 = \frac{1}{\omega_d}\left(\varsigma\omega x_i + \dot{x}_i - \frac{2\varsigma^2 - 1}{\omega^2} + \frac{\varsigma}{\omega}a_i\right) \tag{B.7}$$

$$C_2 = x_i - \frac{2\varsigma}{\omega^3}\frac{\Delta a_i}{\Delta t} + \frac{a_i}{\omega^2}\,. \tag{B.8}$$

Substituting C_1 and C_2 into equation (B.5) and setting $t=t_{i+1}$ leads to the recurrence relationship for x_i and $\dot{x}_i$, given by:

$$\begin{Bmatrix} x_{i+1} \\ \dot{x}_{i+1} \end{Bmatrix} = \left[A(\varsigma,\omega,\Delta t)\right]\begin{Bmatrix} x_i \\ \dot{x}_i \end{Bmatrix} + \left[B(\varsigma,\omega,\Delta t)\right]\begin{Bmatrix} a_i \\ a_{i+1} \end{Bmatrix}. \tag{B.9}$$

The elements of matrices A and B are:

$$\left.\begin{aligned} a_{11} &= e^{-\varsigma\omega\Delta t}\left(\frac{1}{\sqrt{1-\varsigma^2}}\sin\omega_d\Delta t + \cos\omega_d\Delta t\right) \\ a_{12} &= \frac{e^{-\varsigma\omega\Delta t}}{\omega_d}\sin\omega_d\Delta t \\ a_{21} &= -\frac{\omega}{\sqrt{1-\varsigma^2}}e^{-\varsigma\omega\Delta t}\sin\omega_d\Delta t \\ a_{22} &= e^{-\varsigma\omega\Delta t}\left(\cos\omega_m\Delta t - -\frac{1}{\sqrt{1-\varsigma^2}}\sin\omega_d\Delta t\right) \end{aligned}\right\}. \tag{B.10}$$

$$\left.\begin{aligned} b_{11} &= e^{-\varsigma\omega\Delta t}\left[\left(\frac{2\varsigma^2-1}{\omega^2\Delta t}+\frac{\varsigma}{\omega}\right)\frac{\sin\omega_d\Delta t}{\omega_d}+\left(\frac{2\varsigma}{\omega^3\Delta t}+\frac{1}{\omega^2}\right)\cos\omega_d\Delta t\right]-\frac{2\varsigma}{\omega^3\Delta t} \\ b_{12} &= e^{-\varsigma\omega\Delta t}\left[\left(\frac{2\varsigma^2-1}{\omega^2\Delta t}\right)\frac{\sin\omega_d\Delta t}{\omega_d}+\frac{2\varsigma}{\omega^3\Delta t}\cos\omega_d\Delta t\right]-\frac{1}{\omega^2}\frac{2\varsigma}{\omega^3\Delta t} \\ b_{21} &= e^{-\varsigma\omega\Delta t}\left[\left(\frac{2\varsigma^2-1}{\omega^2\Delta t}+\frac{\varsigma}{\omega^2}\right)\left(\cos\omega_d\Delta t-\frac{\varsigma}{\sqrt{1-\varsigma^2}}\sin\omega_d\Delta t\right)\right. \\ &\quad \left.-\left(\frac{2\varsigma^2}{\omega^2\Delta t}+\frac{1}{\omega^2}\right)\left(\omega_d\sin\omega_d\Delta t+\varsigma\omega\cos\omega_d\Delta t\right)\right]+\frac{1}{\omega^2\Delta t} \\ b_{22} &= -e^{-\varsigma\omega\Delta t}\left[\frac{2\varsigma^2-1}{\omega^2\Delta t}\left(\cos\omega_d\Delta t-\frac{\varsigma}{\sqrt{1-\varsigma^2}}\sin\omega_d\Delta t\right)\right. \\ &\quad \left.-\frac{2\varsigma}{\omega^2\Delta t}\left(\omega_d\sin\omega_d\Delta t+\varsigma\omega\cos\omega_d\Delta t\right)\right]-\frac{1}{\omega^2\Delta t} \end{aligned}\right\}. \tag{B.11}$$

Therefore, if the displacement and velocity of the oscillator are known at t_i , the complete response can be computed by a step-by-step application of equation (B.9). The advantage of this method lies in the fact that for a constant time interval Δt, matrices A and B depend only upon ζ and ω, and are constant during the calculation of the response.
To calculate and plot complete response spectra, maximum values of displacement SD = $|x(t)|_{max}$, velocity $SV = |\dot{x}(t)|_{max}$ and absolute acceleration $SA = |\ddot{x}(t) + a(t)|_{max}$ are stored

for each period $T = \frac{2\pi}{\omega}$ and a fraction of critical damping ζ . The calculation of these maxima is approximate because the displacement x(t), velocity $\dot{x}(t)$, and acceleration $\ddot{x}(t)$ are found only at discrete points, where the values are x_i, $\dot{x}_i$, and $\ddot{x}_1 + a_i$ for i = 1,2,…,N (where N is the total number of discrete, equally spaced points at which the input accelerogram is given). For standard spectrum calculations, the choice of the interval of integration ΔT is selected to be:

$$\Delta t \le \frac{T}{10}, \tag{B.12}$$

but it is always less than or equal to Δt_{max} = 0.02 s. Here, T is the period of the oscillator for which the spectrum point is calculated. For such a choice of integration interval the discretization error is always less than 5%.

References for NOTES A and B

Amini, A., and Trifunac, M.D. (1985). "Statistical Extension of Response Spectrum Superpositions," *Soil Dynamics and Earthquake Eng.,* Vol. 4, No. 2, pp. 54-63.

Biot, M.A. (1932). "Vibrations of Buildings During Earthquake," Chapter II in Ph.D. Thesis No. 259, entitled "Transient Oscillations in Elastic System," Aeronautics Department, Calif. Inst. of Tech., Pasadena, California.

Biot, M.S. (1933). "Theory of Elastic Systems Vibrating Under Transient Impulse With an Application to Earthquake-Proof Buildings," *Proc. National Academy of Sciences*, 19(2), pp. 262-268.

Biot, M.A. (1934). "Theory of Vibration of Buildings During Earthquakes," *Zeitschrift für. Angewandte Matematik und Mechanik*, 14(4), pp. 213-223.

Biot, M.A. (1941). "A Mechanical Analyzer for the Prediction of Earthquake Stresses," *Bull. Seism. Soc. Amer*., 31, pp. 151-171.

Biot, M.A. (1942). "Analytical and Experimental Methods in Engineering Seismology," *ASCE Transactions*, 108, 365-408.

Caughey, T. K. (1959). "Classical Normal Modes in Damped Linear Systems," *Journ. App. Mechs*., 59-A-62.

Goodman, L. E., Rosenblueth, E., and Newmark, N.M. (1958). "Seismic Design of Firmly Founded Elastic Structures," *Trans. Amer. Soc. Civil Eng*., 120, pp. 782-802.

Gupta, I.D., and Trifunac, M.D. (1987a). "Statistical Analysis of Response Spectra Method in Earthquake Engineering," *Dept. of Civil Eng. Report No*. CE 87-03 Univ. of Southern California, Los Angeles, California.

Gupta, I.D., and Trifunac, M.D. (1987b). "Order Statistics of Peaks in Earthquake Response of Multi-Degree-of-Freedom Systems," *Earthquake Eng. and Eng. Vibration*, Vol. 7, No. 4, pp. 15-50.

Gupta, I.D., and Trifunac, M.D. (1987c). "Order Statistics of Peaks of Response to Multi-Component Seismic Excitation," *Bull. of Indian Society of Earthquake Technology*, Vol. 24, No. 3-4, pp. 135-159.

Gupta, I.D., and Trifunac, M.D. (1988). "Order Statistics of Peaks in Earthquake Response," *J. Engineering Mechanics*, ASCE, Vol. 114, No. 10, pp. 1605-1537.

Gupta, V.K., and Trifunac, M.D. (1989). "Investigation of Building Response to Translational and Rotational Earthquake Excitations," *Dept. of Civil Eng. Report No. CE 89-02*, Univ. of Southern California, Los Angeles, California.

Hudson, D.E. (1962). "Some Problems in the Application of Spectrum Techniques to Strong-Motion Earthquake Analysis," *Bull. Seism. Soc. Amer*., 52, pp. 417-430.

Jennings, R. L., and Newmark, N.M. (1960). "Elastic Response of Multi-Story Shear Beam Type Structures," *Proc. Second World Conf. On Earthquake Eng*., Tokyo, Vol. II, 699-717.

Kawasumi, H. (1956). "Notes on the Theory of Vibration Analyzer," *Bull. Earthquake Res. lnst*., Tokyo University, Vol. XXXIV, Part I.

Merchant, H. C., and Hudson, D.E. (1962). "Mode Superposition in Multi-Degree-of-Freedom System Using Earthquake Response Spectrum Data," *Bull. Seism. Soc. Amer*., 52, pp. 405-416.

Nigam, N.C., and Jennings, P.C. (1968). "Digital Calculation of Response Spectra From Strong-Motion Earthquake Records," *Earthquake Eng. Res. Lab*., California Institute of Technology, Pasadena.

Rayleigh, J.W. S. (1937). "The Theory of Sound," New York: MacMillan.

Rubin, S. (1961). "Concepts in Shock Data Analysis," Chapter 23 of Shock and Vibration Handbook (ed. C.M. Harris and C.E. Crede), New York: McGraw-Hill.

Trifunac, M.D. (1993). "Broad Band Extension of Fourier Amplitude Spectra of Strong Motion Acceleration" *Dept. of Civil Eng., Report No. CE 93-01*, Univ. of Southern California, Los Angels, California.

Trifunac, M.D. (1995a). "Pseudo-Relative velocity spectra of Earthquake Ground Motion at Long Periods," *Soil Dynam. and Earthqu. Engng*, 14(5), pp. 331-346.

Trifunac, M.D. (1995b). "Pseudo-Relative velocity spectra of Earthquake Ground Motion at High Frequencies," *Earthqu. Engng. and Structural Dynamics*, 24(8), pp. 1113-1130.

Trifunac, M.D. Hudson, D.E., Brady A.G., and Vijayaraghavan, A. (1971). "Strong-Motion Earthquake Accelerograms, II, Corrected Accelerograms and Integrated Velocity and Displacement Curves," *Earthquake Engineering Research Laboratory, Report EERL 71-51*, California Institute of Technology, Pasadena, California.

Von Kármán, T., and Edson, L. (1967). *The Wind and Beyond*, Little, Brown and Co., Boston, Toronto.

Von Kármán, T., and Biot, M.A. (1940) "Mathematical Methods in Engineering," *McGraw-Hill*, New York, London.

.

NOTE C

C. EMPIRICAL SCALING OF RESPONSE SPECTRA (modified from Lee 2007)

By the mid-1960s, when modern digital computers became available, empirical regression analyses of spectral amplitudes were not possible because there were only a few significant processed earthquake records (e.g., those recorded during the 1933 Long Beach, the 1940 Imperial Valley, the 1952 Kern County, the 1966 Parkfield, and the 1968 Borrego Mountain earthquakes). Also, the digitization and processing of strong-motion records from analog instruments was a slow, manual process, requiring many hours of hand digitization (Trifunac, 2006). Response spectra were scaled in terms of peak amplitudes of strong ground motion approximately. For example, Newmark and co-workers (Newmark and Veletsos, 1964; Veletsos et al., 1965) noted that the shape of response spectra can be determined by specifying peak acceleration, peak velocity, and peak displacement of strong ground motion. Spectrum shape was also studied by Blume et al. (1972), who analyzed 33 records. The joint recommendations of the Newmark and Blume studies of the shape of the response spectra (Newmark et al., 1973) were later adopted by the U.S. Atomic Energy Commission (now the U.S. Nuclear Regulatory Commission, USAEC, 1973) for use in the design of nuclear power plants.

The San Fernando earthquake of February 9, 1971 changed all that. More than 250 analog accelerometers in Southern California were triggered and recorded many excellent acceleration traces. The earthquake strong-motion data processing program at the California Institute of Technology in Pasadena, California, led by D.E. Hudson, then started to select, digitize, and process all significant records, and by 1975 all of the records had been processed. The data were then distributed on magnetic tapes and computer cards. A series of reports were published detailing the corrected and processed acceleration, velocity, and displacement of each record, and the corresponding response spectral amplitudes were calculated at 91 periods between 0.04 to 15 seconds for damping ratios of 0.0, 0.02, 0.05, 0.10, and 0.20 (Hudson *et al.*, 1970, 1971 1972a,b).

During the following 30 years, many well-recorded strong-motion earthquakes occurred worldwide, including the three in California: the 1987 Whittier-Narrows, the 1989 Loma-Prieta, and the 1994 Northridge earthquakes. With an ever-increasing digitized database, various groups started to develop regression equations for the empirical scaling of response spectral amplitudes. These equations were later used for the computation of uniform hazard PSV spectra in the probabilistic site-specific analyses for seismic micro- and macro-zonation (Trifunac, 1988, 1989d, 1990b). Those equations were also needed in the probabilistic determination of the envelopes of shear forces and of bending moments in engineering design (Amini and Trifunac, 1985; Gupta and Trifunac, 1988a,b, 1990a,b; Todorovska, 1994a,b,c), and in the estimation of losses for buildings exposed to strong shaking (Jordanovski *et al*., 1993).

Summary of the contributions of the Strong-Motion Group at USC

The Strong-Motion Earthquake Research Group at the University of Southern California contributed papers and reports on the empirical scaling of strong-motion spectra. The examples include:

1970s: Trifunac, 1973; 1976a,b,c; 1977a,b,c,d; 1978; 1979; Trifunac and Anderson, 1977; 1978a,b,c; Trifunac and Brady, 1975a,d,c,d,e; Trifunac and Lee, 1978; 1979a.
1980s: Trifunac and Lee, 1980; 1985a,b,c; 1987; 1989a,b; Lee and Trifunac, 1985; Lee, 1989; Trifunac, 1989a,b,c,d; Trifunac and Todorovska, 1989a,b; Trifunac *et al.,* 1988.
1990s: Lee, 1990; 1991; 1993; Trifunac, 1990a,b; 1991a,b; Trifunac and Lee, 1990; 1992; Trifunac and Novikova, 1994; Lee and Trifunac, 1993; 1995a,b; Lee *et al.*, 1995; Todorovska, 1994a,b,c; Trifunac and Zivcic, 1991; Trifunac *et al.,* 1991.
2000s: Trifunac and Todorovska, 2001a,b.

Three generations of empirical regression equations for the scaling and attenuation of spectral amplitudes have been developed so far. Semi-theoretical extrapolation functions for extension of these empirical equations to both high and low frequencies had also been presented (Trifunac, 1993a,b; 1994a,b,c,d,e; 1995a,b;). A review of and further details on the contributions of this group can be found in Lee (2002). The following is a brief summary of all their work on the empirical scaling of response spectral amplitudes only.

The Database and Data Processing Procedures

The database for the first generation of scaling equations of spectral amplitudes in the 1970s consisted of 186 free-field recordings. This corresponds to 558 acceleration components of data from 57 earthquakes in the western U.S. The data had been selected, digitized, and processed while Trifunac and Lee were at the Engineering Research Laboratory of the California Institute of Technology in Pasadena. The earthquakes included in the list of contributing events started with the 1933 Long Beach earthquake and ended with the San Fernando earthquake of 1971. The magnitudes of the earthquakes in the database ranged from 3.0 to 7.7, and all data were hand digitized from analog records using a manually operated digitizer (Hudson *et al*., 1970, 1971, 1972a,b).

In 1976, the Strong-Motion Group moved to the University of Southern California in Los Angeles. The automatic digitization and data processing of strong-motion records by a mini-computer were developed and introduced in 1979 (Trifunac and Lee, 1979b; Lee and Trifunac, 1979), and the work on the collection of strong-motion records (Anderson *et al.,* 1981; Trifunac and Todorovska, 2001a) continued. By the early 1980s, the second-generation database was expanded to 438 free-field records from 104 earthquakes. Most of the contributing earthquakes were from northern and southern California, and all were from the western U.S. All of these strong-motion records are documented in a series of USC reports entitled the Earthquake Strong-Motion Data Information System (EQINFOS) (Trifunac and Lee, 1987).

By late 1994, the strong-motion database (third generation) grew to over 1,926 free-field records from 297 earthquakes and aftershocks. Those included the records from the main shock and aftershocks of both the 1987 Whittier Narrows and the 1994 Northridge earthquakes in Southern California, and from the 1989 Loma Prieta earthquake in Northern California. Many accelerograms in Southern California were recorded by the USC strong-motion array (Trifunac and Todorovksa, 2001b). If the analog records were available, those were digitized and processed by the automatic digitization system using a PC in the strong-motion laboratory at USC (Lee and Trifunac, 1990). Other records included were mainly those from the Strong-Motion Instrumentation Program (SMIP) of the California Division of Mines and Geology (CDMG) and from the United States Geological Survey.

At each stage of the database processing, all data were treated uniformly, using the standard software for image processing developed at USC (Trifunac and Lee, 1979b; Lee and Trifunac, 1979, 1984).

II. Site Classification

The first geological site classification was introduced (Trifunac and Brady, 1975b) to describe the broad environment of the recording station and was based on geologic maps. The recording sites were to be viewed on a scale measured in terms of kilometers, in contrast to the geotechnical site characterization viewed for the top several tens of meters only (Trifunac, 1990a). This geological site classification is:

Table 1

Geological Site Classification	Description
0	alluvial and sedimentary deposits
1	intermediate sites
2	basement rock

Ideally, according to this approach, a site should be classified either as being on sediments (s = 0) or on the basement rock (s = 2). However, for some sites having a complex environment, an "intermediate" classification (s = 1) was assigned. Trifunac and Lee (1979a) later refined the above classification and used the depth of sediment beneath the recording site, *h*, in km, as a site characteristic. This new parameter was used in the second generation of empirical scaling equations in the 1980s.

In the 1980s, additional parameters were introduced to refine the characterization of the local site beyond the geological site condition, *s*, and the depth of sediments, *h*. The first is the local soil type, s_L, representative of the top 100 ~ 200 m of soil (Trifunac, 1990a).

Table 2

Soil Type, s_L	Description
0	"rock" soil site
1	stiff soil site

2 deep soil site

The second parameter added to site characterization was the average shear wave velocity, V_L, of the soil in the top 30 m. The soil velocity type variable, S_T, was used as follows:

Table 3

Soil Velocity Type, S_T	Description
A	$V_L > 0.75$ km/s
B	$0.75 \geq V_L > 0.36$
C	$0.36 \geq V_L > 0.18$
D	$V_L \leq 0.18$ km/s

In the scaling equations, the velocity type was represented by indicator variables.

III. Distance Definition Used for Attenuation Relation

In the 1970s, the functional form of the attenuation with epicentral distance *R* followed the definition of local magnitude scale (Trifunac, 1976b), which states that the logarithm of the corrected peak amplitude on a standard instrument is equal to the earthquake magnitude (Richter, 1958; Trifunac, 1991b). Hence, the functional form of attenuation,

$$\log A_0(R) + \ldots - g(T)R\,, \tag{C.1}$$

was used, where $\log A_0(R)$ together with a term linear in epicentral distance at each period was intended to account for the average correction for anelastic attenuation. A detailed description of this attenuation function can be found in Trifunac (1976b).

In 1980s, Trifunac and Lee (1985a,b) developed the first magnitude-frequency-dependent attenuation function, $\mathcal{Att}(\Delta, M, T)$, a function of the "representative" distance Δ from the source to the site, for magnitude *M* and for period *T* of strong motion. For a complete, detailed physical description of such a function, the reader is referred to the above reference. Briefly, $\mathcal{Att}(\Delta, M, T) = \mathcal{A}_0(T)\log_{10}\Delta$, where

$$\mathcal{A}_0(T) = \begin{cases} a + b\log_{10} T + c\left(\log_{10} T\right)^2 & T < 1.8\,\text{sec} \\ -0.732025 & T \geq 1.8\,\text{sec} \end{cases} \tag{C.2}$$

with $\mathcal{A}_0(T)$, a function in *T*, approximated by a parabola for $T < 1.8\,\text{sec}$ and a constant beyond that, where $a = -0.767$, $b = 0.272$ and $c = -0.526$. Δ, the source-to-station distance, was defined as in Gusev (1983):

$$\Delta = S\left(\ln\frac{R^2 + H^2 + S^2}{R^2 + H^2 + S_0^2}\right), \tag{C.3}$$

where R is the surface distance from epicenter to the site, H is the focal depth, $S = 0.2 + 8.51(M - 3)$ is the size of the earthquake source at magnitude M, and S_0 is the correlation radius of the source function. It was approximated by $S_0 = c_S T / 2$, where c_S is the shear wave velocity in the rocks surrounding the fault.

In the 1990s, Trifunac and Lee (1990) modified this attenuation function to the following form:

$$\mathcal{Att}(\Delta, M, T) = \begin{cases} \mathcal{A}_0(T) \log_{10}\left(\Delta / L\right) & R \le R_{\max} \\ \mathcal{A}_0(T) \log_{10}\left(\Delta_{\max} / L\right) - \left(R - R_{\max}\right) / 200 & R > R_{\max} \end{cases} \qquad \text{(C.4)}$$

with Δ and R defined as above. $\Delta_{\max}$ and $R_{\max}$ represent the distances beyond which $\mathcal{Att}(\Delta, M, T)$ has a slope defined by the Richter's local magnitude scale M_L. The new parameter, $L = L(M)$, was introduced to model the length of the earthquake fault. It was approximated by $L = .01 \times 10^{0.5M}\ km$ (Trifunac, 1993a,b). Δ / L is thus a dimensionless representative source-to-station distance.

IV. The Source-to-Station Path Types

In the third generation of regression studies of spectral amplitudes in the 1990s, a new term (Lee *et al.,* 1995; Lee and Trifunac, 1995a,b), *r, 0 ≤ r ≤ 1* (or *100r*, as a percentage) was introduced. In this, *r* is the ratio (or percentage) of wave path through geological basement rock relative to the total path, measured along the surface from the earthquake epicenter to the recording site. Alternately, a generalized path type classification was also used. It describes the characteristic types of wave paths between the sources and stations for the strong-motion data available up to the early 1990s in the western U. S.. At that time, due to the limited amount of data, only eight such categories could be identified with a sufficient number of recordings to be included in the regression analyses.

Table 4

Path Type	Description
1.	sediments-to-sediments (100%)
2.	rock-to-sediments, almost vertically
3.	rock-to-sediments, almost horizontally
4.	rock-to-rock (100%)
5.	rock-to-rock through sediments, almost vertically
6.	rock-to-sediments through rock and sediments, almost vertically
7.	rock-to-sediments through rock and sediments, almost horizontally
8.	rock-to-rock through sediments, almost horizontally.

Figure C.1 shows a schematic representation of the "geometry" of these path types. The eight path types in this figure can further be grouped into four path groups: "1", "2", "3", and "4", as described in Table 5.

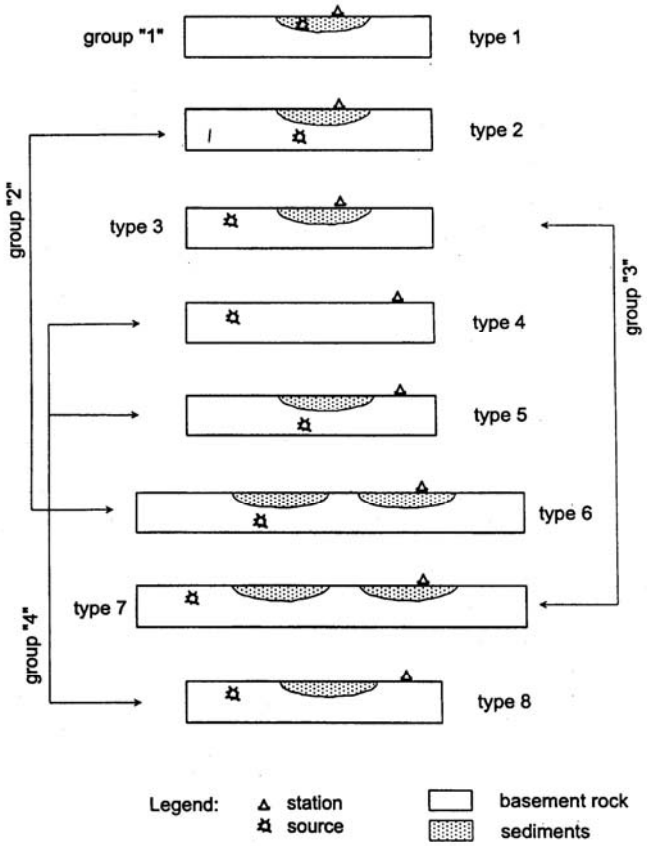

Figure C.1. Eight path types from source to recording station.

Table 5

Path Group	Path Types	Description
"1"	1	Earthquake source and recording site within the same sediment;
"2"	2, 6	Earthquake source in basement rock, recording site almost vertically above;
"3"	3, 7	Earthquake source in basement rock close to the surface; Recording site on nearby sediment, almost horizontally;
"4"	4, 5, 8	Earthquake source in basement rock, recording site on the same basement rock, with or without sediments between.

V. The Scaling Equations

Only the most recent (the third generation) scaling equations (Lee and Trifunac, 1995a,b) for spectral amplitudes will be illustrated here. A description of the complete set of scaling relations of all three generations can be found in Lee (2002). The following regression equations illustrate the four scaling models.

Model (i): Mag-site + soil + % rock path multi-step model

$$\log PSV(T) = \begin{array}{l} M + \mathcal{Att}(\Delta, M, T) + b_1(T)M + b_2(T)s + b_3(T)v + b_4(T) + b_5(T)M^2 \\ \quad + \sum_i b_6^{(i)}(T)S_6^{(i)} + \left(b_{70}(T)r + b_{71}(T)(1-r)\right)R_< \end{array}, \qquad \text{(C.5)}$$

where $R_< = \min\left(R, R_{\max}\right)$, and $\mathcal{Att}(\Delta, M, T)$ were defined in the previous section (Eqn. 4). Substituting $\mathcal{Att}(\Delta, M, T)$ into Eqn. C.5 gives:

$$\log PSV(T) = \begin{cases} M + \mathcal{A}_0(T)\log_{10}\left(\Delta/L\right) + b_1(T)M + b_2(T)s + b_3(T)v + b_4(T) + b_5(T)M^2 \\ \quad + \sum_i b_6^{(i)}(T)S_6^{(i)} + \left(b_{70}(T)r + b_{71}(T)(1-r)\right)R & R \le R_{\max} \\ M + \mathcal{A}_0(T)\log_{10}\left(\Delta_{\max}/L\right) + b_1(T)M + b_2(T)s + b_3(T)v + b_4(T) + b_5(T)M^2 \\ \quad + \sum_i b_6^{(i)}(T)S_6^{(i)} + \left(b_{70}(T)r + b_{71}(T)(1-r)\right)R_{\max} - \dfrac{\left(R - R_{\max}\right)}{200} & R > R_{\max} \end{cases} \qquad \text{(C.6)}$$

Model (ii): Mag-depth + soil + % rock path multi-step model

$$\begin{array}{l} \log PSV(T) = M + \mathcal{Att}(\Delta, M, T) + b_1(T)M + b_2(T)h + b_3(T)v + b_4(T) + b_5(T)M^2 \\ \quad + \sum_i b_6^{(i)}(T)S_6^{(i)} + \left(b_{70}(T)r + b_{71}(T)(1-r)\right)R_< \end{array} \qquad \text{(C.7)}$$

Model (iii): Mag-site + no soil + % rock path multi-step model

$$\begin{array}{l} \log PSV(T) = M + \mathcal{Att}(\Delta, M, T) + b_1(T)M + b_2(T)s + b_3(T)v + b_4(T) + b_5(T)M^2 \\ \quad + \left(b_{70}(T)r + b_{71}(T)(1-r)\right)R_< \end{array} \qquad \text{(C.8)}$$

Model (iv): Mag-site + no soil + % rock path multi-step model

$$\begin{array}{l} \log PSV(T) = M + \mathcal{Att}(\Delta, M, T) + b_1(T)M + b_2(T)h + b_3(T)v + b_4(T) + b_5(T)M^2 \\ \quad + \left(b_{70}(T)r + b_{71}(T)(1-r)\right)R_< \end{array} \qquad \text{(C.9)}$$

Description of the detailed steps required for the development of these regression equations, and illustration of the results and comparison with the actual data can be found

in Lee and Trifunac (1995a,b), a brief summary of which can also be found in Lee (2002).

Note 1:The equations of Lee and Trifunac (1995a,b) (as did all previous USC equations) considered the horizontal and vertical response spectral amplitudes simultaneously in the same equation. These are differentiated by the term $b_3(T)v$, where $v = 0$ for the horizontal components and $v = 1$ for the vertical components.

VI. Scaling With Modified Mercalli Intensity (MMI)

Instead of using magnitude and distance to describe the strong earthquake motions, another alternate scaling parameter is the site intensity. In the U.S., the Modified Mercalli Intensity Scale (MMI) is used. To scale PSV spectra in terms of MMI, I_{MM}, the (first generation) scaling equations can take the following form (Trifunac and Lee, 1979a):

$$\log_{10}\left[PSV(T)\right] = b(T)I_{MM} + c(T) + d(T)h + e(T)v \qquad \text{(C.10)}$$

with I_{MM} being the discrete levels of the MMI scale at the recording site, and all other scaling parameters, *h* and *v,* being the same as before. In the second generation, in the 1980s, the analysis was carried out on the database of 438 free-field records from 104 earthquakes. For some of the free-field sites, the reported MMI levels were not available, so estimated MMI levels were used instead. These estimated MMI levels were calculated using the equation (Lee and Trifunac, 1985):

$$\hat{I}_{MM} = 1.5M - A - B\ln\Delta - C\Delta/100 - Ds \ . \qquad \text{(C.11)}$$

$\hat{I}_{MM}$ was then used in place of I_{MM} in the above scaling equation (C.10).

Comparison with the Work of Several Other Groups and Conclusions

The scaling models of thee other research groups were compared by Lee (2007) with those outlined above, and their differences and similarities discussed. Since a typical scaling model involves the database, the regression parameters, the dependent scaling variables, and the scaling equation used in regression, all these for all the studies have been examined. The reader can further peruse those comparisons in Lee (2007).

References

Amini, A. and Trifunac, M.D. (1985). “Statistical Extension of Response Spectrum Superposition”, Int. J. Soil Dynam. Earthquake Engg., Vol. 4, No. 2, pp. 54–63.

Anderson, J.G., Trifunac, M.D., Amini, A. and Moslem, K. (1981). "Los Angeles Vicinity Strong Motion Accelerograph Network", Department of Civil Engineering, Report CE 81-04, University of Southern Calif., Los Angeles, California.

Blume, J.A., Sharpe, R.L., and Dalal, J.S. (1972). "Recommendations for Shape of Earthquake Response Spectra," S. Francisco,: J. Blume and Associates, AEC Report No. 1254.

Gupta, I.D. and Trifunac, M.D. (1988a). "Order Statistics of Peaks in Earthquake Response", ASCE J. Engng Mech., Vol. 114, No. 10, 1605–1627.

Gupta, I.D. and Trifunac, M.D. (1988b). "Attenuation of Intensity with Epicentral Distance in India", Int. J. Soil Dynamics and Earthquake Eng., Vol. 7, 162–169.

Gupta, I.D. and Trifunac, M.D. (1990a). "Probabilistic Spectrum Superposition for Response Analysis Including the Effects of Soil-Structure Interaction", J. Prob. Engg. Mech., Vol. 5, No. 1, 9–18.

Gupta, V.K. and Trifunac, M.D. (1990b). "Response of Multistoried Buildings to Ground Translation and Rocking During Earthquakes", J. Prob. Engg. Mech., Vol. 5, No. 3, 138–145.

Gusev, A.A. (1983). "Descritpive Statistical Model of Earthquake Source Radiation and Its Application to An Estimation of Short-Period Strong Motion", Geoph. J. Royal Astro. Soc., Vol. 74, 787–808.

Hudson, D.E., Trifunac, M.D. and Brady, A.G. (1970). "Strong-Motion Earthquake Accelerograms, Digitized and Plotted Data, Vol. I", Earthquake Engineering Research Laboratory, EERL 70-20, California Institute of Technology, Pasadena.

Hudson, D.E., Trifunac, M.D., Brady, A.G. and Vijayaraghavan, A. (1971). "Strong-Motion Earthquake Accelerograms, II, Corrected Accelerograms and Integrated Velocity and Displacement Curves", Earthquake Engineering Research Laboratory, EERL 71-50, California Institute of Technology, Pasadena.

Jordanovski, L.R., Lee, V.W., Manic, M.I., Olumceva, T., Sinadinovski, C., Todorovska, M.I. and Trifunac, M.D. (1987). "Strong Earthquake Ground Motion Data in EQINFOS: Yugoslavia, Part I", Civil Eng. Report CE 87-05, Univ. of Southern Cal., Los Angeles.

Jordanovski, L.R., Todorovska, M.I. and Trifunac, M.D. (1993). "Total Loss in a Building Exposed to Earthquake Hazard, Part I: The Model; Part II: A Hypothetical Example", Europ. Earthqu. Engng, Vol. VI, No. 3, 14–32.

Lee, V.W. (1989). "Empirical Scaling of Pseudo Relative Velocity Spectra of Recorded Strong Earthquake Motion in Terms of Magnitude and Both Local Soil and Geologic Site Classifications", Earthqu. Engng and Engng Vib., Vol. 9, No. 3, 9–29.

Lee, V.W. (1990). "Scaling PSV Spectra in Terms of Site Intensity, and Both Local Soil and Geological Site Classifications", Europ. Earthqu. Engng, Vol. IV, No. 3, 3–12.

Lee, V.W. (1991). "Correlation of Pseudo Relative Velocity Spectra with Site Intensity, Local Soil Classification and Depth of Sediments", Soil Dynam. Earthqu. Engng., Vol. 10, No. 3, 141–151.

Lee, V.W. (1993). "Scaling PSV from Earthquake Magnitude, Local Soil and Geological Depth of Sediments", ASCE J. Geotech. Engng, Vol. 119, No. 1, 108–126.

Lee, V.W. (2002). "Empirical Scaling of Strong Earthquake Ground Motion: Part I: Attenuation and Scaling of Response Spectra", ISET J. Earthquake Technology, Vol. 39, No. 4, 219–254.

Lee, V.W. (2007). Empirical Scaling and Regression Methods for Earthquake Strong-Motion Spectra – A Review, *Indian Soc. of Earthquake Technology J.,* **44**(1), (in press).

Lee, V.W. and Trifunac, M.D. (1979) "Automatic Digitization and Data Processing of Strong-Motion Accelerograms, Part II: Computer Processing of Accelerograms ", Civil Eng. Report CE 79-15II, Univ. of Southern Cal., Los Angeles.

Lee, V.W. and Trifunac, M.D. (1984). "Current Developments in Data Processing of Strong-Motion Accelerograms ", Civil Eng. Report CE 84-01, Univ. of Southern Cal., Los Angeles.

Lee, V.W. and Trifunac, M.D. (1985). "Attenuation of Modified Mercalli Intensity for Small Epicentral Distance in California", Civil Eng. Report CE 85-01, Univ. of Southern California, Los Angeles, CA.

Lee, V.W. and Trifunac, M.D. (1990). "Automatic Digitization and Data Processing of Accelerograms Using PC ", Civil Eng. Report CE 90-03, Univ. of Southern Cal., Los Angeles, CA.

Lee, V.W. and Trifunac, M.D. (1993). "Empirical Scaling of Fourier Amplitude Spectra in Former Yugoslavia", Europ. Earthqu. Engng, Vol. VII, No. 2, 47–61.

Lee, V.W. and Trifunac, M.D. (1995a). "Frequency Dependent Attenuation Function and Fourier Amplitude Spectra of Strong Earthquake Ground Motion in California", Report CE 95-03, Dept. of Civil Eng., Univ. of Southern California, Los Angeles, CA.

Lee, V.W. and Trifunac, M.D. (1995b). "Pseudo Relative Velocity Spectra of Strong Earthquake Ground Motion in California", Report CE 95-04, Dept. of Civil Eng., Univ. of Southern California, Los Angeles, CA.

Lee, V.W., Trifunac, M.D., Todorovska, M.I. and Novikova, E.I. (1995). "Empirical Equations Describing Attenuation of the Peaks of Strong Ground Motion, in Terms of Magnitude, Distance, Path Effects, and Site Conditions", Report CE 95-02, Dept. of Civil Eng., Univ. of Southern California, Los Angeles, CA.

Newmark, N.M., and Veletsos, A.S. (1964). "Design Procedures for Shock Isolation Systems of Underground Protective Structures," Vol. III, Response Spectra of Single-Degree-of-Freedom Elastic and Inelastic Systems," Report for Air Force Weapons Laboratory, by Newmark, Hansen and Associates, RTD TDR 63-3096.

Newmark, N.M., Blume, J.A., and Kapur, K.K. (1973). "Seismic Design Criteria for Nuclear Power Plants," *J. of the Power Division, ASCE*, Vol. 99, pp. 287-303.

Richter, C.F. (1958). "Elementary Seismology", Freeman and Co., San Francisco.

Todorovska, M.I. (1994a). "A Note on Distribution of Amplitudes of Peaks in Structural Response Including Uncertainties of the Exciting Ground Motion and of the Structural Model", Soil Dynam. Earthqu. Engng, Vol. 14, No. 3, 211–217.

Todorovska, M.I. (1994b). "Order Statistics of Functionals of Strong Motion", Soil Dynam. Earthqu. Engng, Vol. 13, No. 3, 149–161.

Todorovska, M.I. (1994c). "Comparison of Response Spectrum Amplitudes from Earthquakes with Lognormally and Exponentially Distributed Return Period", Soil Dynam. Earthqu. Engng., Vol. 13, No. 1, 97–116.

Trifunac, M.D. (1973). "Analysis of Strong Earthquake Ground Motion for Prediction of Response Spectra", Int. J. Earthqu. Engng Struct. Dynam., Vol. 2, No. 1, 59–69.

Trifunac, M.D. (1976a). "Preliminary Analysis of the Peaks of Strong Earthquake Ground Motion—Dependence of Peaks on Earthquake Magnitude, Epicentral Distance and Recording Site Conditions", Bull. Seism. Soc. Amer., Vol. 66, 189–219.

Trifunac, M.D. (1976b). "Preliminary Empirical Model for Scaling Fourier Amplitude Spectra of Strong Ground Acceleration in Terms of Earthquake Magnitude, Source to Station Distance and Recording Site Conditions", Bull. Seism. Soc. Amer., Vol. 68, 1345–1373.

Trifunac, M.D. (1976c). "A Note on the Range of Peak Amplitudes of Recorded Accelerations, Velocities and Displacements with Respect to the Modified Mercalli Intensity", Earthquake Notes, Vol. 47, No. 1, 9–24.

Trifunac, M.D. (1978). "Response Spectra of Earthquake Ground Motion", ASCE J. Eng. Mech., Vol. 104, No. 5, 1081–1097.

Trifunac, M.D. (1979). "Preliminary Empirical Model for Scaling Fourier Amplitude Spectra of Strong Motion Acceleration in Terms of Modified Mercalli Intensity and Geologic Site Conditions", Int. J. Earthqu. Engng and Struct. Dynam., Vol. 7, 63–74.

Trifunac, M.D. (1988). "Seismic Microzonation Mapping via Uniform Risk Spectra", Proc. 9th World Conf. Earthqu. Engng, Tokyo-Kyoto, Japan, Vol. VII, 75–80.

Trifunac, M.D. (1989a). "Dependence of Fourier Spectrum Amplitudes of Recorded Strong Earthquake Accelerations on Magnitude, Local Soil Conditions and on Depth of Sediments", Int. J. Earthquake Eng. Structural Dyn., Vol. 18, No. 7, 999–1016.

Trifunac, M.D. (1989b). "Empirical Scaling of Fourier Spectrum Amplitudes of Recorded Strong Earthquake Accelerations in Terms of Magnitude and Local Soil and Geologic Site Conditions", Earthquake Eng. Eng. Vibration, Vol. 9, No. 2, 23–44.

Trifunac, M.D. (1989c). "Scaling Strong Motion Fourier Spectra by Modified Mercalli Intensity, Local Soil and Geologic Site Conditions", Structural Eng./Earthquake Eng., JSCE, Vol. 6, No. 2, 217–224.

Trifunac, M.D. (1989d). "Threshold Magnitudes Which Exceed the Expected Ground Motion during the Next 50 Years in a Metropolitan Area", Geofizika, Vol. 6, 1–12.

Trifunac, M.D. (1990a). "How to Model Amplification of Strong Earthquake Motions by Local Soil and Geologic Site Conditions", Earthqu. Engng Struct. Dynam., Vol. 19, No. 6, 833–846.

Trifunac, M.D. (1990b). "A Microzonation Method Based on Uniform Risk Spectra", Soil Dynam. Earthqu. Engng, Vol. 9, No. 1,
34–43.

Trifunac, M.D. (1991a). "Empirical Scaling of Fourier Spectrum Amplitudes of Recorded Strong Earthquake Accelerations in Terms of Modified Mercalli Intensity, Local Soil Conditions and Depth of Sediments", Int. J. Soil Dynamics Earthquake Eng., Vol. 10, No. 1, 65–72.

Trifunac, M.D. (1991b). "*MSM ",* Int. J. Soil Dynam. Earthqu. Engng, Vol. 10, No. 1, 17–25.

Trifunac, M.D. (1993a). "Long Period Fourier Amplitude Spectra of Strong Motion Acceleration", Soil Dynam. Earthqu. Engng, Vol. 12, No. 6, 363–382.

Trifunac, M.D. (1993b). "Broad Band Extension of Fourier Amplitude Spectra of Strong Motion Acceleration", Report CE 93-01, Dept. of Civil Eng., Univ. of Southern California, Los Angeles, CA.

Trifunac, M.D. (1994a). "Fourier Amplitude Spectra of Strong Motion Acceleration: Extension to High and Low Frequencies", Earthqu. Engng Struct. Dynam., Vol. 23, No. 4, 389–411.

Trifunac, M.D. (1994b). "*Q* and High Frequency Strong Motion Spectra", Soil Dynam. Earthqu. Engng, Vol. 13, No. 4, 149–161.

Trifunac, M.D. (1994c). "Earthquake Source Variables for Scaling Spectral and Temporal Characteristics of Strong Ground Motion", Proc. 10th Europ. Conf. Earthqu. Eng., Vienna, Austria, Vol. 4, 2585–2590.

Trifunac, M.D. (1994d). "Response Spectra of Strong Motion Acceleration: Extension to High and Low Frequencies", Proc. 10th Europ. Conf. Earthqu. Eng., Vienna, Austria. Vol. I, 203–208.

Trifunac, M.D. (1994e). "Broad Band Extension of Pseudo Relative Velocity Spectra of Strong Motion", Report CE 94-02, Dept. of Civil Eng., Univ. Southern California, Los Angeles, CA.

Trifunac, M.D. (1995a). "Pseudo Relative Velocity Spectra of Earthquake Ground Motion at Long Periods", Soil Dynam. Earthqu. Engng, Vol. 14, No. 5, 331–346.

Trifunac, M.D. (1995b). "Pseudo Relative Velocity Spectra of Earthquake Ground Motion at High Frequencies", Earthqu. Engng Struct. Dynam., Vol. 24, No. 8, 1113–1130.

Trifunac, M.D. (2006). "Brief History of Computation of Earthquake Response Spectra", Soil Dynam. Earthqu. Engng, Vol. 26, 501–508.

Trifunac, M.D. and Anderson, J.G. (1977). "Preliminary Empirical Models for Scaling Absolute Acceleration Spectra", Report CE 77-03, Dept. of Civil Eng., Univ. of Southern California, Los Angeles, CA.

Trifunac, M.D. and Anderson, J.G. (1978a). "Preliminary Empirical Models for Scaling Pseudo Relative Velocity Spectra", Report CE 78-04, Dept. of Civil Eng., Univ. of Southern California, Los Angeles, CA.

Trifunac, M.D. and Anderson, J.G. (1978b). "Preliminary Models for Scaling Relative Velocity Spectra", Report CE 78-05, Dept. of Civil Eng., Univ. of Southern California, Los Angeles, CA.

Trifunac, M.D. and Anderson, J.C. (1978c). "Estimation of Relative Velocity Spectra", Proc. 6th Symp. Earthquake Engineering, University of Roorkee, India.

Trifunac, M.D. and Brady, A.G. (1975a). "A Study on the Duration of Strong Earthquake Ground Motion", Bull. Seism. Soc. Amer., Vol. 65, 581–626.

Trifunac, M.D. and Brady, A.G (1975b). "On the Correlation of Seismic Intensity Scales with the Peaks of Recorded Strong Ground Motion", Bull. Seism. Soc. Amer., Vol. 65, 139–162.

Trifunac, M.D. and Brady, A.G. (1975c). "On the Correlation of Seismoscope Response with Earthquake Magnitude and Modified Mercalli Intensity", Bull. Seism. Soc. Amer., Vol. 65, 307–321.

Trifunac, M.D. and Brady, A.G. (1975d). "Correlations of Peak Acceleration, Velocity and Displacement with Earthquake Magnitude, Epicentral Distance and Site Conditions", Int. J. Earthquake Engineering Struct. Dynamics, Vol. 4,
455–471.

Trifunac, M.D. and Brady, A.G. (1975e). "On the Correlation of Peak Accelerations of Strong-Motion with Earthquake Magnitude, Epicentral Distance and Site Conditions" Proc. U.S. National Conference Earthquake Engineering, Ann Arbor, MI., 43–52.

Trifunac, M.D. and Lee, V.W. (1978). "Dependence of Fourier Amplitude Spectra of Strong Motion Acceleration on the Depth of Sedimentary Deposits", Report CE 78-14, Dept. of Civil Eng., Univ. of Southern California, Los Angeles, CA.

Trifunac, M.D. and Lee, V.W. (1979a). "Dependence of Pseudo Relative Velocity Spectra of Strong Motion Acceleration on the Depth of Sedimentary Deposits", Report CE 79-02, Dept. of Civil Eng., Univ. of Southern California, Los Angeles, CA.

Trifunac, M.D. and Lee, V.W. (1979b). "Automatic Digitization and Data Processing of Strong-Motion Accelerograms, Part I: Automatic Digitization", Report CE 79-15 I, Dept. of Civil Eng., Univ. of Southern California, Los Angeles, CA.

Trifunac, M.D. and Lee, V.W. (1985a). "Frequency Dependent Attenuation of Strong Earthquake Ground Motion", Report CE 85-02, Dept. of Civil Eng., Univ. of Southern California, Los Angeles, CA.

Trifunac, M.D. and Lee, V.W. (1985b). "Preliminary Empirical Model for Scaling Fourier Amplitude Spectra of Strong Ground Acceleration in Terms of Earthquake Magnitude, Source to Station Distance, Site Intensity and Recording site Conditions", Report CE 85-03, Dept. of Civil Eng., Univ. of Southern California, Los Angeles, CA.

Trifunac, M.D and Lee, V.W. (1985c). "Preliminary Empirical Model for Scaling Pseudo Relative Velocity Spectra of Strong Earthquake Acceleration in Terms of Magnitude,

Distance, Site Intensity and Recording Site Conditions", Report CE 85-04, Dept. of Civil Eng., Univ. of Southern California, Los Angeles, CA.

Trifunac, M.D. and Lee, V.W. (1987). "Direct Empirical Scaling of Response Spectral Amplitudes from Various Site and Earthquake Parameters", Report NUREG/CE-4903, U.S. Nuclear Regulatory Commission, Vol. I.

Trifunac, M.D. and Lee, V.W. (1990). "Frequency Dependent Attenuation of Strong Earthquake Ground Motion", Int. J. Soil Dynam. Earthqu. Engng, Vol. 9, No. 1, 3–15.

Trifunac, M.D. and Lee, V.W. (1992). "A Note on Scaling Peak Acceleration, Velocity and Displacement of Strong Earthquake Shaking by Modified Mercalli Intensity (MMI) and Site Soil and Geologic Conditions", Soil Dynamics Earthquake Eng., Vol. 11, No. 2, pp. 101–110.

Trifunac, M.D. and Novikova, E.I. (1994). "State of the Art Review of Strong Motion Duration", Proc. 10th Europ. Conf. Earthqu. Eng., Vienna, Austria, Vol. 1, 131–140.

Trifunac, M.D. and Todorovska, M.I. (1989a). "Attenuation of Seismic Intensity in Albania and Yugoslavia", Int. J. Struct. Dynamics Earthquake Eng., Vol. 10, No. 5, 617–631.

Trifunac, M.D. and Todorovska, M.I. (1989b). "Methodology for Selection of Earthquake Design Motions for Important Engineering Structures", Report CE 89-01, Dept. of Civil Eng., Univ. Southern Calif., Los Angeles, CA.

Trifunac, M.D. and Todorovska, M.I. (2001a). "A Note on the Useable Range in Accelerographs Recording Translation", Soil Dynamics Earthquake Eng., Vol. 21, No.4, 275–286.

Trifunac, M.D. and Todorovska, M.I. (2001b). "Evolution of Accelerographs, Data Processing, Strong Motion Arrays and Amplitude and Spatial Resolution in Recording Strong Earthquake Motion", Soil Dynamics Earthquake Eng., Vol. 21, No. 6, 537–555.

Trifunac, M.D. and Zivcic, M. (1991). "A Note on Instrumental Comparison of the Modified Mercalli Intensity (MMI) in the Western United States and the Mercalli-Cancani-Sieberg (MCS) Intensity in Yugoslavia", European Earthquake Eng., Vol. V, No. 1, 2–26.

Trifunac, M.D., Lee, V.W., Cao, H. and Todorovska, M.I. (1988). "Attenuation of Seismic Intensity in Balkan Countries", Report CE 88-01, Dept. of Civil Eng., Univ. of Southern Calif., Los Angeles, CA.

Trifunac, M.D., Lee, V.W., Zivcic, M. and Manic, M. (1991). "On the Correlation of Mercalli-Cancani-Sieberg Intensity Scale in Yugoslavia with the Peaks of Recorded Strong Earthquake Ground Motion", European Earthquake Eng., Vol. V, No. 1, 27–33.

United States Atomic Energy Commission (1973). "Design Response Spectra for Seismic Design of Nuclear Power Plants," Regulatory Guide No. 1.60, U.S. Atomic Energy Commission, Washington, D.C.

..

NOTE D

D. DESIGN SPECTRA

Fixed-Shape Response Spectra

In his 1934 paper, Biot stated: "If we possessed a great number of seismogram spectra we could use their envelope as a standard spectral curve for the evaluations of the probable maximum effect on buildings." In Biot (1941a), he continued: "These standard curves … could be made to depend on the nature and magnitude of the damping and on the location. Although the do not lead to final results, we … conclude that the spectrum will generally be a function decreasing with the period for values of the latter greater than about 0.2 s. A standard curve for earthquakes of the Helena and Ferndale … for values T > 0.2 s, could very well be the simple hyperbola $A = \frac{0.2g}{T}$ and for T < 0.2 s, A = g(4T + 0.2), where T is the period in seconds and g the acceleration of gravity (this standard spectrum is plotted in Figures D.1 through D.4). Whether this function would fit other earthquakes can only be decided by further investigations."

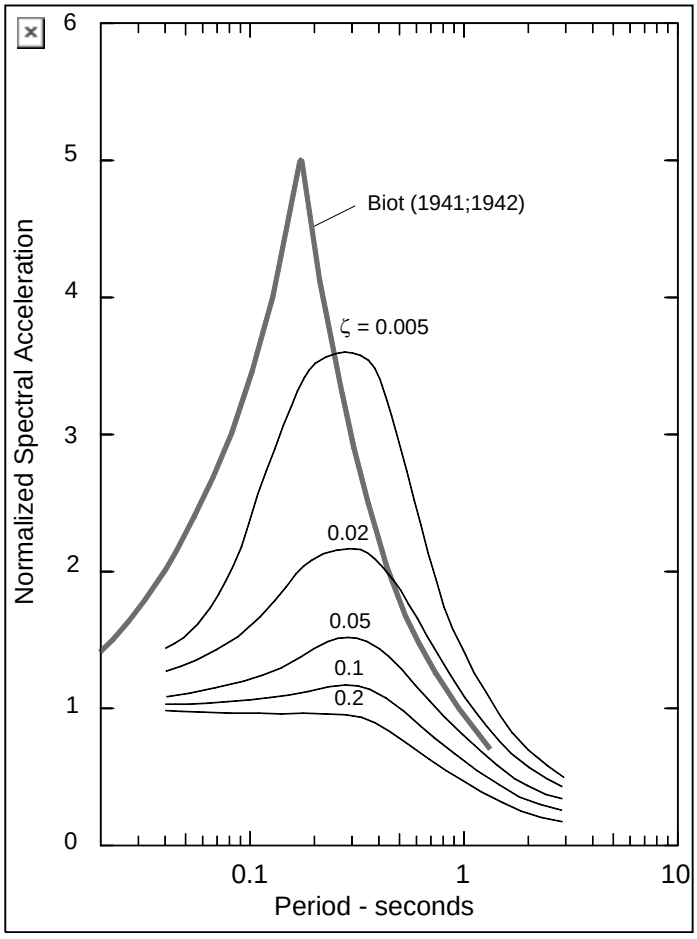

Fig. D.1 Comparison of Biot (1941; 1942) "standard spectrum" (heavy line) with average spectrum of Housner (1959, 1970).

Fifteen years later, Housner averaged and smoothed the response spectra of three strong-motion records from California (El Centro, 1934, M = 6.5; El Centro, 1940, M = 6.7; and Tehachapi, 1952, M = 7.7) and one from Washington (Olympia, 1949, M = 7.1) He advocated the use of this average spectrum shape in earthquake engineering design (Fig. D.1, Housner, 1959; 1970).

Newmark and co-workers (Newmark and Veletsos, 1964; Veletsos et al., 1965) noted that the shape of response spectra can be determined by specifying peak acceleration, peak velocity, and peak displacement of strong ground motion. Spectrum shape was further studied by Mohraz et al. (1972) using 14 strong-motion records and by Blume et al. (1972), who analyzed 33 records. The joint recommendations of the Newmark and Blume studies of the shape of the response spectra (Newmark et al., 1973) were later adopted by the U.S. Atomic Energy Commission (now the U.S. Nuclear Regulatory Commission, USAEC, 1973) for use in the design of nuclear power plants (Fig. D.2).

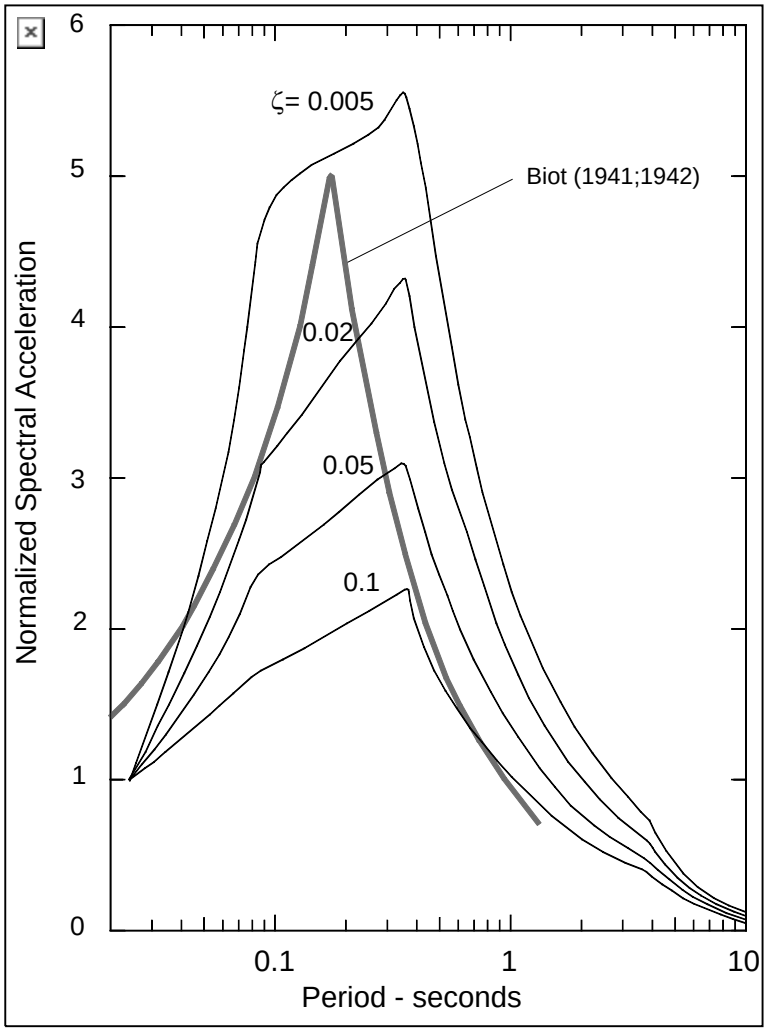

Fig. D.2 Comparison of Biot (1941; 1942) "standard spectrum" (heavy line) with regulatory guide 1.60 spectrum (USAEC, 1973).

In engineering design work, the fixed shapes of Housner and Newmark spectra, normalized to unit peak acceleration, were scaled by selecting the "design" peak acceleration. This procedure, which was first systematically used in the design of nuclear power plants, emerged as the "standard" scaling procedure for determination of design spectra in the late 1960s and early 1970s.

Site-Dependent Spectral Shapes

In one of the first studies to consider the site-dependent shape of earthquake response spectra, Hayashi et al. (1971) averaged spectra from 61 accelerograms in three groups, according to the recording site conditions (A – very dense sands and gravels; B – soils with intermediate characteristics, and C – very loose soils), and showed that the soil site condition has an effect on the shape of average response spectra. This result was later confirmed by Seed et al. (1976), who considered 104 records and four site conditions (rock, stiff soil, deep cohesionless soil, and soft-to-medium clay and sand; Fig. D.3).

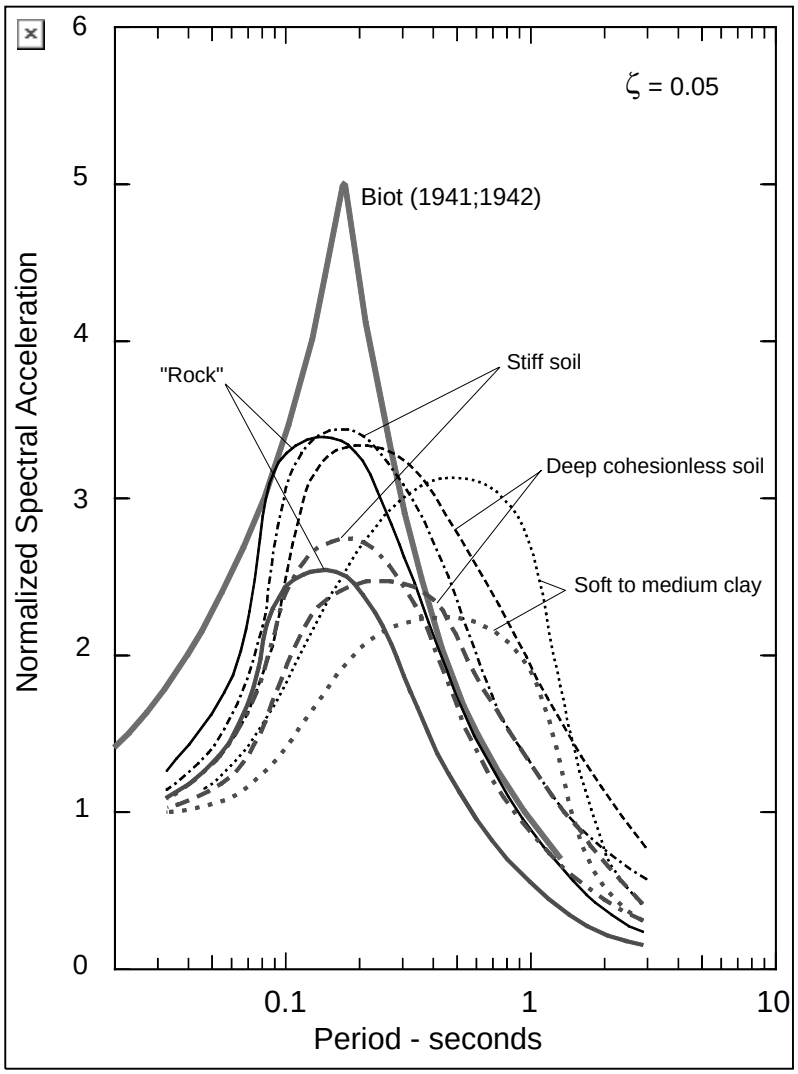

Fig. D.3 Comparison of Biot (1941; 1942) "standard spectrum" (heavy line) with average (heavy lines) and average plus standard deviation spectra (light lines) of Seed et al. (1976) for four soil site conditions.

Mohraz et al. (1972) suggested that the peak ground displacement, d, and peak ground velocity, v, were d = 36 in. and v = 48 in./s for "alluvium" sites and d = 12 in. and v = 28 in./s for "rock" sites, both corresponding to a 1g peak ground Because of the small number of recorded accelerograms on rock in 1972, conclusive recommendations on how to describe the dependence of spectra on site conditions did not appear possible at that time.

A major and persistent problem in the evaluation of site-dependent spectra of strong earthquake motion is the lack of generally accepted procedures on how to characterize a site. Gutenberg (1957) studied the amplification of weak earthquake motions in the Los Angeles area and published the results on average trends and amplification of peak wave

motions in sedimentary basins for periods of motion longer than about 0.5 s. His site characterization could be termed "geological," because he considered the "site" on the scale of kilometers and used the term "rock" to represent geological basement rock. Twenty years later, Gutenberg's results were shown to be in excellent agreement with the empirical scaling of Fourier amplitude spectra of strong-motion accelerograms of 186 records (Trifunac, 1976). While it is clear today that both geotechnical and geological site characterizations must be considered simultaneously (Trifunac, 1990; Lee and Trifunac, 1995), there is so far no general consensus on how to do this.

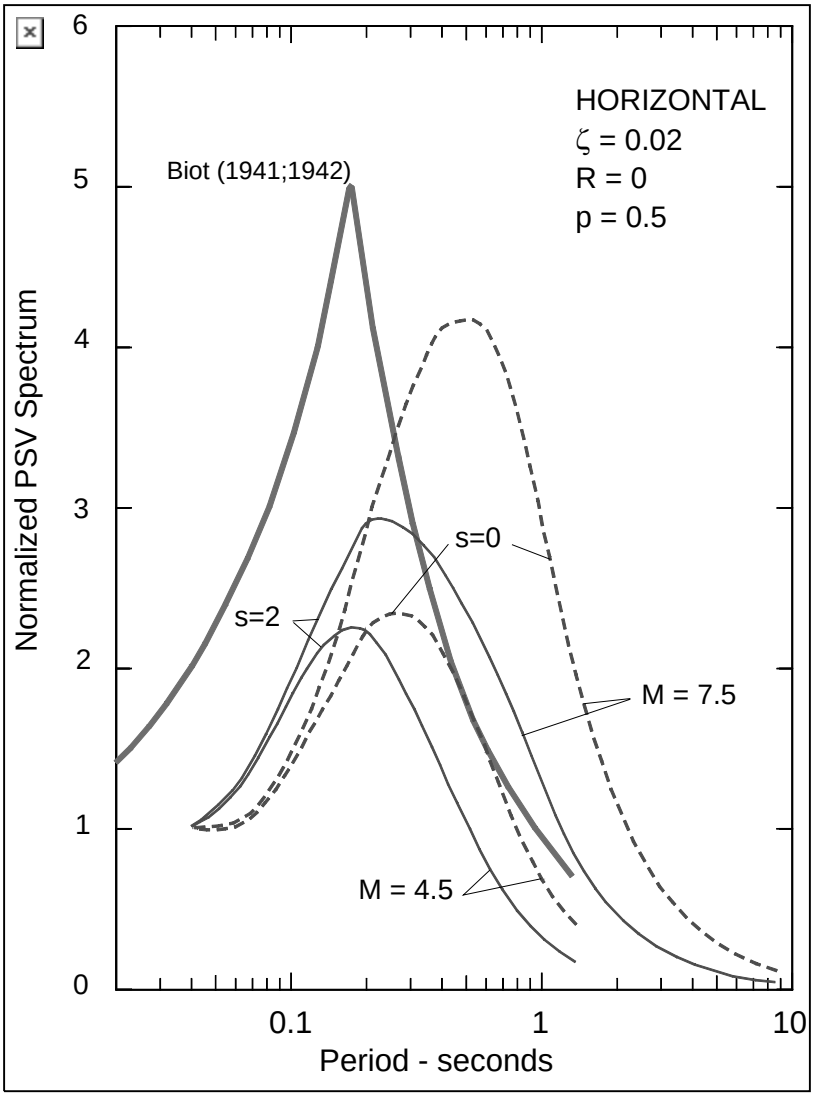

Fig. D.4 Comparison of Biot (1941; 1942) "standard spectrum" (heavy line) with spectral shapes, which depend on magnitude (M = 4.5 and 7.5) and geological site conditions (s = 2 for basement rock and s = 0 for sediments), for average spectral amplitudes (p = 0.5), at zero epicentral distance (R = 0) and for 2 percent of critical damping (ζ = 0.02; Trifunac, 1978).

Site-, Magnitude-, and Distance-Dependent Spectra

The occurrence of the San Fernando, California earthquake in 1971 and the large number of new recordings it contributed to the strong-motion database (Hudson, 1976) opened a new chapter in the empirical studies of earthquake response spectra. For the first time, it became possible to consider multi-parametric regressions and to search for the trends in recorded strong-motion data. It became possible to show how spectral amplitudes and

spectrum shape change, not only with local soil and geologic site conditions, but also with earthquake magnitude and source-to-station distance (Fig. D.4; Trifunac, 1978). During the following 20 years, the subsequent regression studies evolved into advanced empirical scaling equations, contributing numerous detailed improvements and producing a family of advanced, direct-scaling equations for spectral amplitudes in terms of almost every practical combination of scaling parameters. The literature on this subject is voluminous, and its review is beyond the scope of this paper. The readers can find many examples and a review of this subject in Lee (2002).

Figures D.1 through D.4 compare Biot's "standard" spectrum shape with other examples of fixed (Figs. D.1, D.2, and D.3) and variable (Fig. D.4) spectral shapes. These comparisons are only qualitative, because the methods used in their development and the intended use of the spectral shapes differ. Biot's spectrum was originally thought to correspond to zero damping, but it was later discovered that it has small variable damping, probably less than 3 percent of critical. It was based on the spectra of two earthquakes only (Helena, Montana, 1935, M = 6.0, and Ferndale, California, 1934, M = Lee, V.W. (2002). "Empirical Scaling of Strong Earthquake Ground Motion-Part I: Attenuation and Scaling of Response Spectra," *Indian Society of Earthquake Technology Journal*, Vol.39, No.4, pp. 6.4). Housner (Fig. D.1), NRC (Fig. D.2), and Seed et al. (Fig. D.3) spectra were based on progressively larger numbers of recorded accelerograms (4, 33, and 104, respectively) and on recordings during large earthquakes. Therefore they have broader spectral shapes. The variable shape spectrum in Figure D.4 shows only the dependence of spectral shape (normalized to 1-g acceleration) on magnitude and geological site conditions, but it does show clearly how the spectra broaden with increasing magnitude and how larger magnitudes contribute larger long-period spectral amplitudes.

References

Biot, M.A. (1934). "Theory of Vibration of Buildings During Earthquakes," *Zeitschrift für. Angewandte Matematik und Mechanik*, 14(4), pp. 213–223.

Biot, M.A. (1941). "A Mechanical Analyzer for the Prediction of Earthquake Stresses," *Bull. Seism. Soc. Amer.*, 31, pp. 151–171.

Biot, M.A. (1942). "Analytical and Experimental Methods in Engineering Seismology," *ASCE Transactions*, 108, 365-408.

Blume, J.A., Sharpe, R.L., and Dalal, J.S. (1972). "Recommendations for Shape of Earthquake Response Spectra," S. Francisco,: J. Blume and Associates, AEC Report No. 1254.

Gutenberg, B. (1957). "Effects of Ground on Earthquake Motion," *Bull. Seism. Soc. Amer.*, Vol. 47, No. 3, pp. 221–250.

Hayashi, S.H., Tsuchida, H., and Kurata, E. (1971). "Average Response Spectra for Various Subsoil Conditions," *Third Joint Meeting of U.S. Japan Panel on Wind and Seismic Effects*, UJNR, Tokyo.

Housner, G.W. (1959). "Behavior of Structures During Earthquakes," *J. of Eng. Mechanics Division, ASCE*, Vol. 85, No. EM 4, pp. 109–129.

Housner, G.W. (1970). "Design Spectrum," Chapter 5 in *Earthquake Engineering*, New Jersey: R.L Wiegel, Prentice-Hall.

Hudson, D.T. (1976). "Strong-Motion Earthquake Accelerograms," Index Volume, *Earthquake, Eng. Research Lab., EERL* 76–02, Calif. Inst. of Tech., Pasadena, California.

Lee, V.W., and Trifunac, M.D. (1995). "Pseudo Relative velocity spectra of Strong Earthquake Ground Motion in California," *Dept. of Civil Eng., Report No. CE 95–04*, Univ. of Southern California, Los Angeles, California.

Mohraz, B., Hall, W.J., and Newmark, N.K. (1972). "A Study of Vertical and Horizontal Earthquake Spectra," *N.M. Newmark Consulting Engineering Services*, Urbana, Illinois: AEC Report No. WASH–1255.

Newmark, N.M., and Veletsos, A.S. (1964). "Design Procedures for Shock Isolation Systems of Underground Protective Structures," Vol. III, Response Spectra of Single-Degree-of-Freedom Elastic and Inelastic Systems," Report for Air Force Weapons Laboratory, by Newmark, Hansen and Associates, RTD TDR 63–3096.

Newmark, N.M., Blume, J.A., and Kapur, K.K. (1973). "Seismic Design Criteria for Nuclear Power Plants," *J. of the Power Division, ASCE*, Vol. 99, pp. 287–303.

Seed, H.B., Ugas, C., and Lysmer, J. (1976). "Site-Dependent Spectra for Earthquake-Resistant Design," *Bull Seismol. Soc. Am.*, Vol. 66, No. 1, pp. 221–243.

Trifunac, M.D. (1976). "Preliminary Empirical Model for Scaling Fourier Amplitude Spectra of Strong Ground Acceleration in Terms of Earthquake Magnitude, Source to Station Distance and Recording Site Conditions," *Bull Seism Soc. Amer.*, Vol. 66, No. 4, pp. 1343–1373.

Trifunac, M.D. (1978). "Response Spectra of Earthquake Ground Motion," *ASCE, EMS*, Vol. 104, pp. 1081–1097.

Trifunac, M.D. (1990). "How to Model Amplification of Strong Earthquake Motions by Local Soil and Geologic Site Conditions," *Earthquake Eng. and Structural Dynamics*, Vol. 19, No. 6, pp. 833–846.

United States Atomic Energy Commission (1973). "Design Response Spectra for Seismic Design of Nuclear Power Plants," Regulatory Guide No. 1.60, U.S. Atomic Energy Commission, Washington, D.C.

Veletsos, A.S., Newmark, N.M., and Chelapati, C.V. (1965). "Deformation Spectra for Elastic and Elasto-Plastic Systems Subjected to Ground Shock and Earthquake Motions," *Proc. of Third World Conf. on Earthquake Eng.,* New Zealand, Vol. II, pp. 663–680.

.

NOTE E

E. UNIFORM HAZARD SPECTRA

For a given earthquake direct empirical scaling produces a response spectrum with amplitude and shape, which depend on the size and distance to the event, on the propagation path, and on the local geologic and soil conditions. In one of the oldest methods for selection of design criteria for important structures, a *scenario* approach, considers the possible contributing events (typically not more than 5 or 6). The design

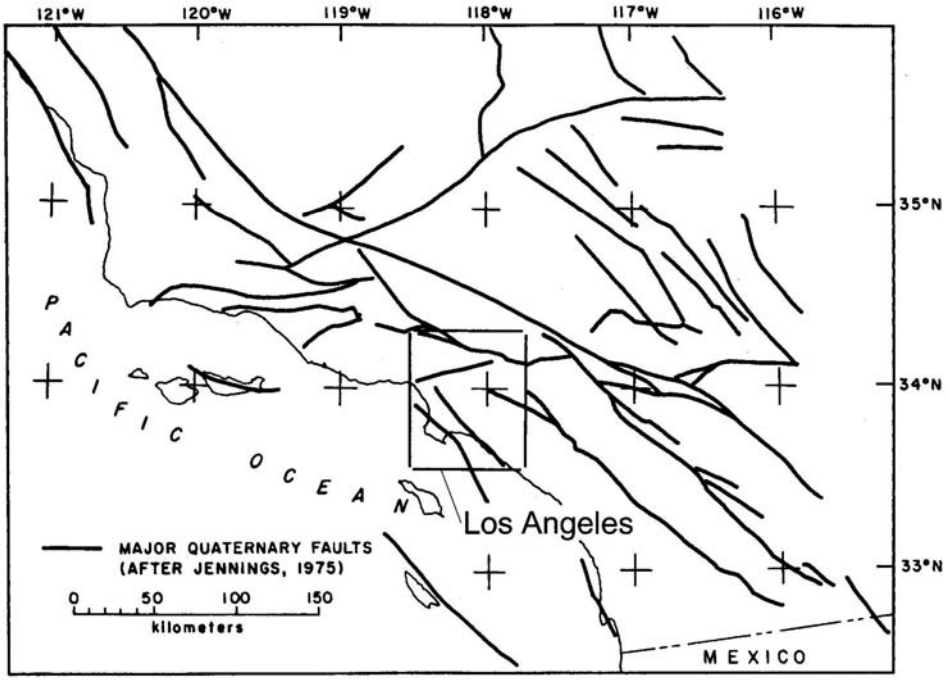

Fig. E.1. Major Quaternary Faults, surrounding Los Angeles area, in Southern California.

spectrum is then chosen to envelope the spectra from all those contributing events. The same concept of enveloping the spectra of the contributing events has been employed in the formulation of the classical design spectral shapes (see Note D). After further amplitude and shape modifications, which are frequently not based on the physical properties of strong motion, but on the judgment of the committees, the shape and the amplitudes of spectral shapes used in design codes, are also, albeit indirectly, based on the scenario approach. This approach works reasonably well for intermediate and distant sites (say for distances greater than 50 km from an earthquake), but can lead to unbalanced representation of strong shaking close to earthquake sources and for large

strong motion amplitudes. Furthermore the basic scenario approach typically does not consider the likelihood of occurrence of a given earthquake event, and this creates a situation where the spectra which serve as a basis for development of the spectral envelopes do not have proper weighting factors. These difficulties can all be eliminated by use of Uniform Hazard Spectrum methodology.

The concept of Uniform Hazard Spectrum (UHS) was introduced in late 1970s (Anderson and Trifunac 1977). UHS is calculated from the distribution functions of all possible

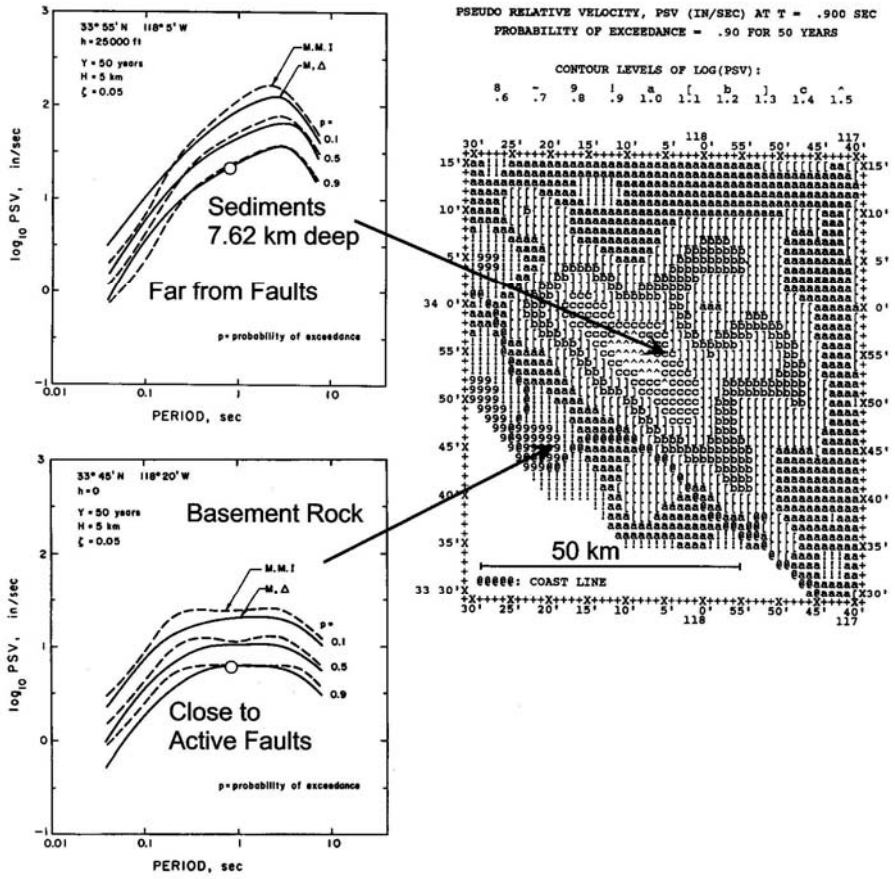

Fig. E.2. (right). Spatial variations of Pseudo Relative Velocity Spectrum amplitudes, at T=0.90 s, for probability of being exceeded equal to 0.90, during exposure of 50 years, to Southern California seismicity (see Fig. E.1). Spectral amplitudes, read from this map, are shown by open circles in the two figures on the left. From a catalogue of figures on the right, for many different periods, and probabilities of being exceeded (Lee and Trifunac 1987) one can construct the two figures on the left. It is seen that the amplitudes and the shape of the Uniform Hazard Spectrum can vary appreciably over short distances, due to the geological site conditions and proximity of the active faults.

spectral amplitudes, during specified exposure time (typically 50 years), and by considering all known active earthquake sources within 350 to 450 km radius

surrounding the cite. The methodology was originally developed for use in the design of nuclear power plants, but then gradually became the principal tool in seismic hazard mapping and for advanced site-specific estimates of the consequences of strong shaking (Lee and Trifunac 1987; Todorovska and Trifunac 1996; 1999; Todorovska et al. 2007). Todorovska et al (1995) and Gupta (2007) present comprehensive reviews of the method and many examples of how UHS method can be used.

Fig. E.1 shows the faults in Southern California, surrounding the Los Angeles metropolitan area. By calculating UHS, in this example for PSV amplitudes, at a dense matrix of points, for different probabilities of being exceeded, and for a given exposure period (50 years in this example), UHS amplitudes can be read from a series of maps, and URS spectra can be plotted as illustrated in the left two examples in Fig.E.2. It is seen that the UHS of PSV can change amplitudes and shape over relatively small distances, in this case less than 25 km (Lee and Trifunac 1987).

References

Anderson, J.G. and M.D. Trifunac (1977). On Uniform Risk Functionals which Describe Strong Ground Motion: Definition, Numerical Estimation, and an Application to the Fourier Amplitude Spectrum of Acceleration, Report No. CE77-02, Dept. of Civil Eng, Univ. of Southern California, Los Angeles, USA.

Gupta, I.D. (2007). Probabilistic Seismic Hazard Analysis Method for Mapping of various Parameters to Estimate the Earthquake Effects on Manmade Structures, *Indian Society of Earthquake Technology Journal,* 44(1), (in press).

Lee, V.W. and M.D. Trifunac (1987). Microzonation of A Metropolitan Area, Report No. 87-02, Dept. of Civil Eng., Univ. of Southern California, Los Angeles, USA

Todorovska, M.I., Gupta, I.D., Gupta, V.K., Lee, V.W. and Trifunac, M.D. (1995). Selected Topics in Probabilistic Seismic Hazard Analysis, Report CE 95-08, Dept. of civil Eng., Univ. of Southern California, Los Angeles, USA.

Todorovska, M.I. and M.D. Trifunac (1996). Hazard mapping of normalized peak strain in soil during earthquakes: microzonation of a metropolitan area, Soil Dyn. and Earthq. Eng., **15**(5), 321-329.

Todorovska, M.I. and M.D. Trifunac (1999). Liquefaction opportunity mapping via seismic wave energy, Jour. of Geotech and Geoenvironmental Eng., ASCE, **125**(12), 1032-1042.

Todorovska, M.I., Trifunac, M.D., and Lee, V.W. (2007). Shaking Hazard Compatible Methodology for Probabilistic Assesment of Permanent Ground Displacement Across Earthquake Faults, *Soil Dynamics and Earthquake Engineering*, **27**(6), 586-597 .

NOTE F

F. RESPONSE SPECTRUM AND DESIGN CODES (modified from Freeman 2007)

Work on developing building codes began in Italy in 1908, following the Messina disaster in which more than 100,000 persons were killed; in Japan following the 1923 Tokyo disaster, in which more than 150,000 perished; and in California after the Santa Barbara earthquake of 1925 (Freeman, 1932, Suyehiro, 1932). In 1927, the "Palo Alto Code," developed with the advice of Professors Willis and Marx of Stanford University, was adopted in Palo Alto, San Bernardino, Sacramento, Santa Barbara, Klamath, and Alhambra, all in California. It specified the use of a horizontal force equivalent to 0.1 g, 0.15 g and 0.2 g acceleration on hard, intermediate, and soft ground, respectively.

"Provisions Against Earthquake Stresses," contained in the Proposed U.S. Pacific Coast Uniform Building Code was prepared by the Pacific Coast Building Officials Conference and adopted at its 6th Annual Meeting, in October, 1927, but these provisions were not generally incorporated into municipal building laws (Freeman, 1932). The code recommended the use of horizontal force equivalent to 0.075, 0.075, and 0.10 g acceleration on hard, intermediate, and soft ground, respectively. Following the 1933 Long Beach earthquake, the Field Act was implemented. Los Angeles and many other cites adopted an 8 percent g base shear coefficient for buildings and a 10 percent g for school buildings. In 1943 the Los Angeles Code was changed to indirectly take into account the natural period of vibration.

San Francisco's first seismic code ("Henry Vensano" code) was adopted in 1948, with lateral force values in the range from 3.7 to 8.0 percent of g, depending upon the building height (EERI Oral History Series: Blume, 1994a; Degenkolb, 1994b). Vensano code called for higher earthquake coefficients than were then common in Northern California, and higher than those prescribed by the Los Angeles 1943 code. Continued opposition by San Francisco area engineers led to a general consensus-building effort, which resulted in the "Separate 66" report in 1951. "Separate 66" was based on Maurice Biot's response spectrum calculated for the 1935 Helena, Montana earthquake (The EERI Oral History Series: Housner, 1997; Proc. ASCE, vol. 77, Separate No. 66, April 1951).

In Los Angeles, until 1957 (for reasons associated with urban planning, rather than earthquake safety, and to prevent development of downtown "canyons"), no buildings higher than 150 feet (13-story height limit) could be built. In 1957, the fixed height limit was replaced by the limit on the amount of floor area that could be built on a lot. After the San Fernando, California earthquake of 1971, Los Angeles modified the city code in 1973 by requiring dynamic analysis for buildings over 16 stories high (160 feet).
In 1978, the Applied Technology Council (ATC) issued its ATC-3 report on the model seismic code for use in all parts of the United States. This report, written by 110 volunteers working in 22 committees, incorporated many new concepts, including "more

realistic ground motion" intensities. Much of the current Uniform Building Code was derived from ATC-3 report.

Influence of Response Spectra on Building Code Provisions (from Freeman 2007)

The basis for the development of current seismic building code provisions had their beginnings in the 1950s. A Joint Committee of the San Francisco Section of ASCE and the Structural Engineers Association of Northern California prepared a "model lateral force provision" based on a dynamic analysis approach and response spectra (Anderson et al, 1952). The Proposed Design Curve, $C = K / T$, was based on a compromise between a Standard Acceleration Spectrum by M. A. Biot (Biot 1941, 1942) and the analysis of El Centro accelerogram by E. C. Robison (Figure F.1). It is interesting to note that the Biot curve PGA of 0.2g has a peak spectral acceleration of 1.0g at a period of 0.2 seconds. The curve then descends in proportion to 1/T (i.e., constant velocity). If the peak spectral acceleration is limited to 2.5 times the PGA, the Biot spectrum is very close to the 1997 UBC design spectrum for a PGA of 0.2g (dashed line without symbols in Figure F.1). The proposed design lateral force coefficient was $C = 0.015 / T$, with a maximum of 0.06 and minimum of 0.02 (line with dots in Figure F.2). These values were considered consistent with the current practice and the weight of the building included a percentage of live load.

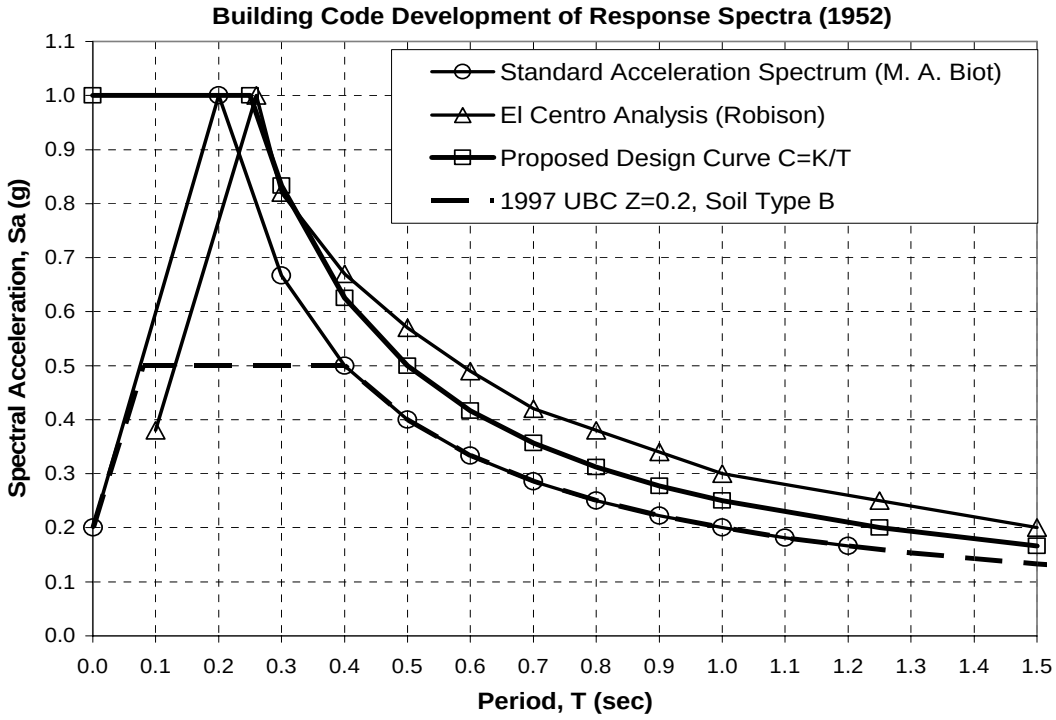

Fig. F.1 1952 Joint Committee (Anderson et al. 1952)

In 1959, the Seismology Committee of the Structural Engineers Association of California published "Recommended Lateral Force Requirements" (generally referred to as the SEAOC bluebook) and included "Commentary" in 1960 (SEAOC 1960). Influenced by the Joint Committee (many of the members were on both committees), recommendations were proposed that were adopted for the 1961 Uniform Building Code (UBC) (ICBO 1961). The new recommended design lateral force coefficient was $C = 0.05/T^{1/3}$ and the live loads were not included in the weight (except for a percentage in storage facilities). By using T to the one-third power, the equation could account for higher modal participation and give a larger load factor for tall buildings. In addition it avoided the need for a minimum cut-off. The maximum was set at $C = 0.10$ (Figure F.2). Also shown in Figure F.2 is a comparably adjusted version of the 1997 UBC.

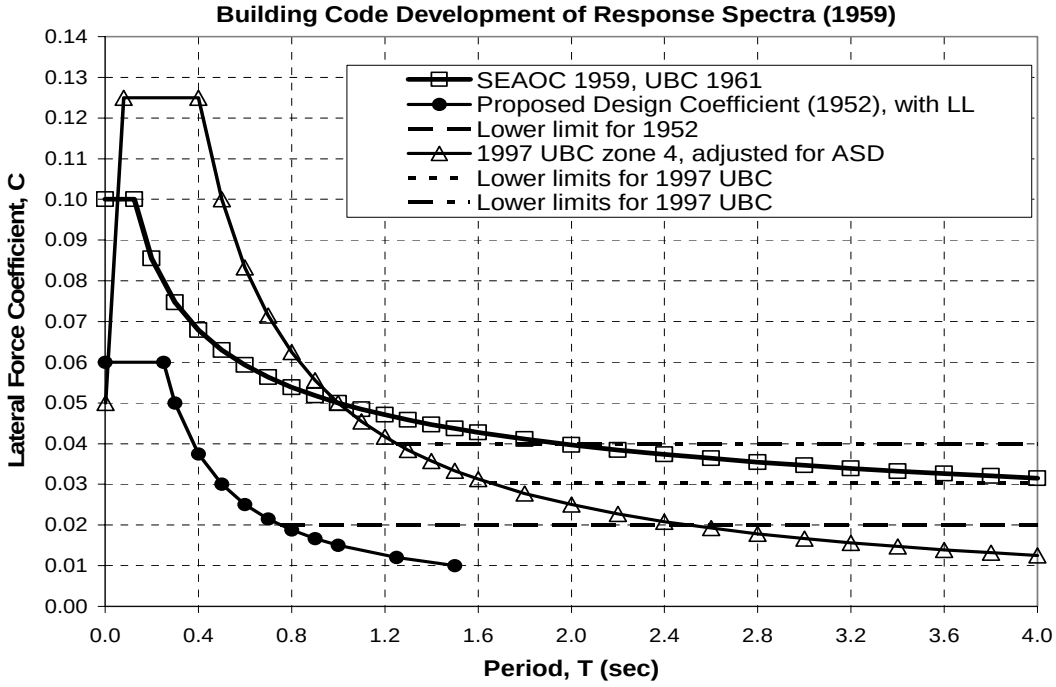

Fig. F.2 1959 code development (SEAOC 1960)

Over the years, the SEAOC bluebook and the UBC went through many revisions, generally influenced by some event such as the 1971 San Fernando, 1989 Loma Prieta, and 1994 Northridge earthquakes and by data relating to soil effects. The comparable curves shown in Figure F.3 have been adjusted to represent strength design response spectra and include factors representing soil classification type D. At this level of design, the structures would be expected to remain linear-elastic with some reserve capacity before reaching yield. In order to survive major earthquake ground motion (e.g., $PGA = 0.4g$) the structure is expected to experience nonlinear post yielding response.

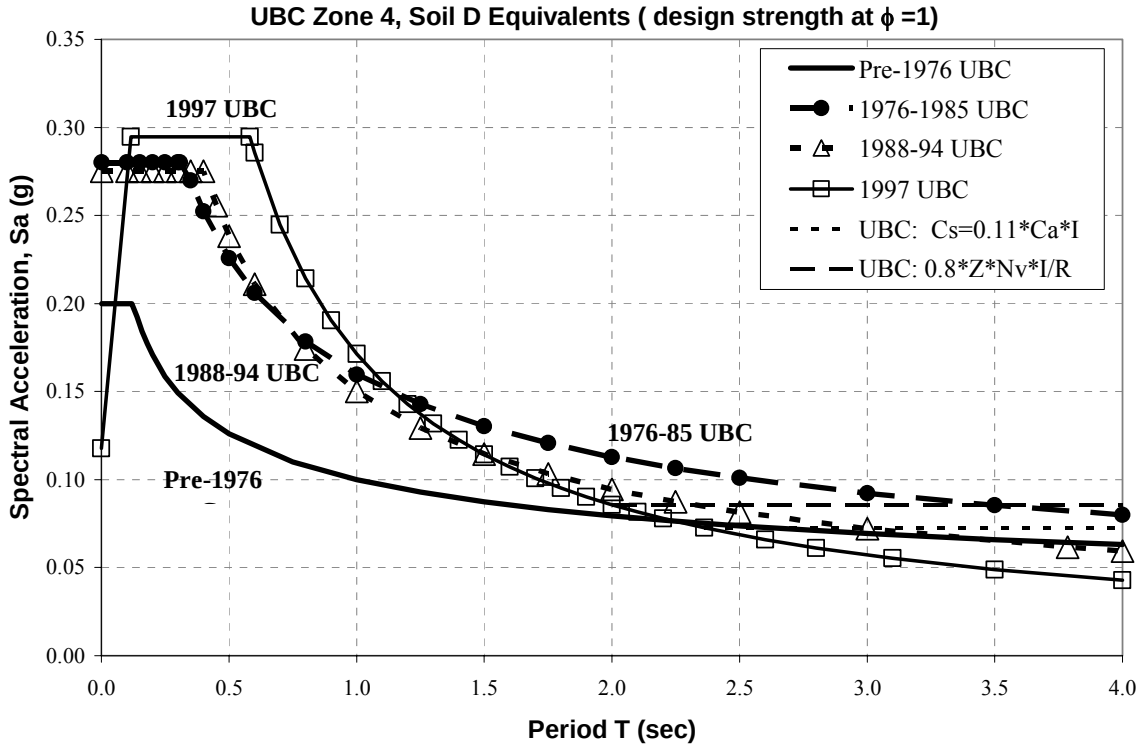

Fig. F.3 UBC response spectra - 1961 to 1997

References

Anderson, A.W., J.A. Blume, H.J. Degenkolb, H.B. Hammill, E.M. Knapik, H.L. Marchand, H.C. Powers, J.E. Rinne, G.A. Sedgwick, and H.O. Sjoberg, (1952). "Lateral Forces of Earthquake and Wind", Transactions of ASCE, Volume 117, 716-780.

Biot, M.A. (1941). "A Mechanical Analyzer for the Prediction of Earthquake Stresses," *Bull. Seism. Soc. Amer.*, 31, 151–171.

Biot, M.A. (1942). "Analytical and Experimental Methods in Engineering Seismology," *ASCE Transactions*, 108, 365–408.

Earthquake Engineering Research Institute (1994a). "Connections, The EERI Oral History Series: J.A. Blume, Stanley Scott Interviewer," *EERI*, 499 14th Street, Suite 320, Oakland, CA 94612.

Earthquake Engineering Research Institute (1994b). "Connections, The EERI Oral History Series: H.J. Degenkolb, Stanley Scott Interviewer," *EERI*, 499 14th Street, Suite 320, Oakland, CA 94612.

Earthquake Engineering Research Institute (1997). "Connections, The EERI Oral History Series: G.W. Housner, Stanley Scott Interviewer," *EERI*, 499 14th Street, Suite 320, Oakland, CA 94612.

Freeman, J.R. (1932). "Earthquake Damage and Earthquake Insurance," New York: McGraw-Hill.

Freeman, S.A. (2007). Response Spectra as a useful Design and Analysis Tool for Practicing Structural Engineers, *ISET Journal of Earthquake Technology*, **44**(1), (in press).

ICBO (1961 et al), "Uniform Building Code (UBC)," by International Conference of Building Officials (ICBO), Whittier, California; 1961-1997.

SEAOC (1960). "Recommended Lateral Force Requirements and Commentary" (Blue Book), Seismology Committee, Structural Engineers Association of California, San Francisco, California.

Suyehiro, K. (1932). "Engineering Seismology Notes on American Lectures," *Proc. ASCE*, Vol. 58, No. 4, 1-110.

.

NOTE G

G. Advanced Vibrational representations of Response

The basic model employed to describe the response of a simple structure to only horizontal earthquake ground motion, $\ddot{\Delta}_x$ is the single-degree-of-freedom system (SDOF) experiencing rocking ψ_r, relative to the normal to the ground surface, and assuming that the ground does not deform in the vicinity of the foundation, that is, neglecting the soil structure interaction (Fig. G.1). Rotation ψ_r is restrained by a spring with stiffness K_r, and by a dashpot with the rocking damping constant C_r, providing the fraction of critical damping ς_r. The natural frequency of this system is $\omega_r = \left(K_r / h^2 m_b\right)^{1/2}$, and for small rocking angles it is governed by the linear ordinary differential equation

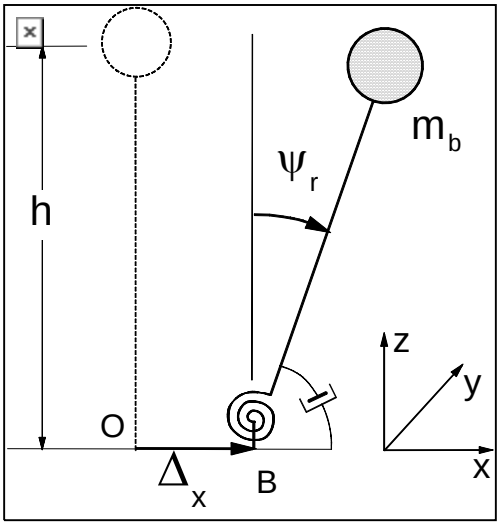

Fig. G.1 Single-Degree-of-Freedom System

$$\ddot{\psi}_r + 2\omega_r \varsigma_r \dot{\psi}_r + \omega_r^2 \psi_r = -\ddot{\Delta}_x / h \qquad \text{(G.1)}$$

For any initial conditions, and for arbitrary excitation this system always leads to deterministic and predictable response. Eqn. (G.1) was used originally to develop the concept of the relative response spectrum, and continues to this day as the main vehicle in formulation of most earthquake engineering analyses of response (Trifunac 2003). If the gravity force is considered, the ω_r in Eq. (G.1) has to be reduced (Biot 2006), and the system becomes metastable for ψ_r smaller than its critical value. At the critical value of ψ_r, the overturning moment of gravity force is just balanced by the elastic moment in the restraining spring.

In more advanced vibrational representations of the response, additional components of earthquake excitation, dynamic instability, soil-structure interaction, spatial and temporal variations of excitation, differential motions at different support points, and nonlinear behavior of the stiffness K_r can be considered, but the structure usually continues to be modeled by mass-less columns, springs, dashpots, and with rigid mass m_b. In the following we illustrate some of the above examples.

Dynamic instability. An example of a simple model, which includes instability is shown in Fig. G.2. It has horizontal vertical and rocking excitations, which can result from

incident P and SV waves, for example. The structure is represented by an equivalent single-degree-of-freedom system, with a concentrated mass m_b at a height h above the foundation. It has a radius of gyration r_b and a moment of inertia $I_b = m_b r_b^2$ about O. The degree-of-freedom in the model of a structure is chosen to correspond to the relative rocking ψ_r. This rotation is restrained by a spring with rocking stiffness K_r and by a dashpot with rocking damping C_r (both not shown in Fig. G.2). The gravitational force $m_b g$ is considered. Taking moments about B results in the equation of motion

$$\ddot{\phi}_y + \ddot{\psi}_r + 2\omega_r \varsigma_r \dot{\psi}_r + \omega_r^2 \psi_r = \left\{ -\left(\ddot{\Delta}_x / a\right)\cos\left(\phi_y + \psi_r\right) + \left(\omega_r^2 \varepsilon_g + \ddot{\Delta}_z / a\right)\sin\left(\phi_y + \psi_r\right) \right\} / \varepsilon \quad \text{(G.2)}$$

where $\varepsilon = h\left(1 + \left(r_b / h\right)^2\right)/a$, $\omega_r^2 = K_r / \left[m\left(h^2 + r_b^2\right)\right]$ is the natural frequency of rocking squared, ζ_r is a fraction of the critical damping in $2\omega_r \varsigma_r = C_r / \left[m\left(h^2 + r_b^2\right)\right]$, and $\varepsilon_g = 2/\omega_r^2 a$. Eqn. (G.2) is a differential equation coupling the rocking of the foundation and the structure with the horizontal and vertical motions of the foundation. It is a nonlinear equation, whose solution will require numerical analysis. In this example we will discuss only the case when $\phi_y + \psi_r$ is small. Then

$$\ddot{\psi}_r + 2\omega_r \varsigma_r \dot{\psi}_r + \left\{ \omega_r^2 \left(1 - \varepsilon_g / \varepsilon\right) - \ddot{\Delta}_z / \varepsilon a \right\} \psi_r = -\ddot{\phi}_y + \left\{ -\ddot{\Delta}_x / a + \left(\omega_r^2 \varepsilon_g + \ddot{\Delta}_z / a\right)\phi_y \right\} / \varepsilon \quad \text{(G.3)}$$

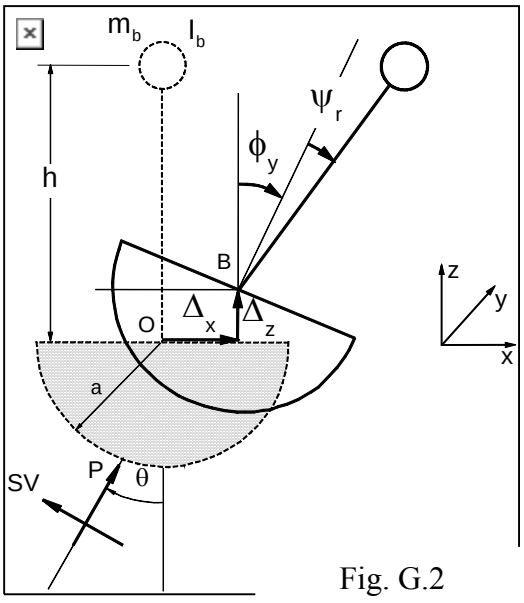

Fig. G.2

For steady-state excitation by incident P and SV waves, with frequency ω, Δ_x, ϕ_y, and Δ_z, and therefore the coefficients of (G.3), will be periodic. Equation (G.3) is then a special form of Hill's equation. Analysis of the stability of this equation can be found in the work of Lee (1979). For general earthquake excitation Δ_x, ϕ_y, and Δ_z will be determined by the recorded components of motion, and in the predictive analyses by simulated ground motions (Lee and Trifunac 1985; 1987; Wong and Trifunac 1979).

In Eqn. (G.3) ϕ_y describes rocking of the foundation to which the structure is attached. In the analyses, which do not consider soil-structure interaction, ϕ_y will be determined directly by the rocking component of strong ground motion (Lee and Trifunac 1987; Jalali and Trifunac 2007). In the studies, which consider soil-structure interaction, ϕ_y will be one of the variables to be determined by the analysis (Lee 1979).

Soil-Structure Interaction. The linear soil-structure interaction embodies the phenomena, which result from (1) the presence of an inclusion (foundation, Fig. G.3) in the half space (Lee and Trifunac 1982), and (2) from the vibration of the structure which is supported by the foundation and which exerts dynamic forces on the foundation (Lee 1979). Examples and a discussion of non-linear aspects of soil-structure interaction can be found in Gicev (2005), and in a review of observations of response to earthquake shaking in full-scale structures in Trifunac et al. (2001a,b,c).

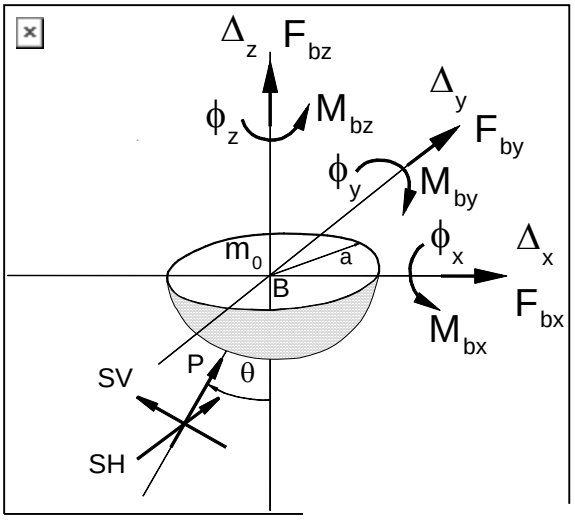

Fig. G.3

The dynamic response of a rigid embedded foundation to seismic waves can be separated into two parts. The first part corresponds to the determination of the restraining forces due to the rigid body motion of the inclusion. The second part deals with the evaluation of the driving forces due to the scattering of incident waves by the inclusion, which is presumed to be immobile. This can be illustrates by considering a foundation embedded in an elastic medium and supporting an elastic superstructure. The steady-state harmonic motion of the foundation having frequency ω can be described by a vector $\{\Delta_x, \Delta_y, \Delta_x, \phi_x, \phi_y, \phi_z\}^T$ (Fig. G.3), where Δ_x and Δ_y are horizontal translations, Δ_z is vertical translation, ϕ_x and ϕ_y are rotations about horizontal axes, and ϕ_z is torsion about the vertical axis. Using superposition, displacement of the foundation is the sum of two displacements

$$\{U\} = \{U^*\} + \{U_0\} \tag{G.4}$$

where $\{U^*\}$ is the foundation input motion corresponding to the displacement of the foundation under the action of the incident waves in the absence of external forces, and $\{U_0\}$ is the relative displacement corresponding to the displacement of the foundation under the action of the external forces in the absence of incident wave excitation.

The interaction force $\{F_s\}$ generates the relative displacement $\{U_0\}$. It corresponds to the force that the foundation exerts on the soil, and it is related to $\{U_0\}$ by $\{F_s\} = [K_s(\omega)]\{U_0\}$, where $[K_s(\omega)]$ is the 6 x 6 complex stiffness matrix of the embedded foundation. It depends upon the material properties of the soil medium, the characteristics and shape of the foundation, and the frequency of the harmonic motion. It describes the force-displacement relationship between the rigid foundation and the soil medium.

The driving force of the incident waves is equal to $\{F_s^*\} = [K_s]\{U^*\}$, where the input motion $\{U*\}$ is measured relative to an inertial frame. The "driving force" is the force that the ground exerts on the foundation when the rigid foundation is kept fixed under the action of incident waves. It depends upon the properties of the foundation and the soil and on the nature of excitation.

The displacement $\{U\}$ is related to the interaction and driving forces via $[K_s]\{U\} = \{F_s\} + \{F_s^*\}$.

For a rigid foundation having a mass matrix $[M_0]$ and subjected to a periodic external force, $\{F_{ext}\}$, the dynamic equilibrium equation is

$$[M_0]\{\ddot{U}\} = -\{F_s\} + \{F_{ext}\}. \qquad \text{(G.5)}$$

$\{F_{ext}\} = \{F_{bx}, F_{by}, F_{bz}, M_{bx}, M_{by}, M_{bz}\}$ is the force the structure exerts on the foundation (Fig. G.3). Then Eqn. (5) becomes

$$[M_0]\{\ddot{U}\} + [K_s]\{U\} = \{F_s^*\} + \{F_{ext}\} \qquad \text{(G.6)}$$

The solution of $\{U\}$ requires the determination of the mass matrix, the impedance matrix, the driving forces and the external forces (Lee 1979).

After the mass matrix $[M_0]$, the stiffness matrix $[K_s]$, and the force $\{F_s^*\}$ have all been evaluated, those can be used to determine the foundation displacement $\{U\}$. For in-plane response, excited by P and SV waves, for example, the relative response ψ_r is then given by the Eqn. (G.3)

Differential motions. Common use of the response spectrum method and many dynamic analyses in earthquake engineering implicitly assume that all points of building foundations move synchronously and with the same amplitudes. This, in effect, implies that the wave propagation in the soil is neglected. Unless the structure is long (e.g., a bridge with long spans, a dam, a tunnel) or "stiff" relative to the underlying soil, these simplifications are justified and can lead to a selection of approximate design forces, if the effects of soil-foundation interaction in the presence of differential ground motions can be neglected (Bycroft, 1980). Simple analyses of two-dimensional models of long buildings suggest that when $a/\lambda < 10^{-4}$, where a is wave amplitude and λ is the *corresponding* wavelength, the wave propagation effects on the response of simple structures can be neglected (Todorovska and Trifunac, 1990).

Figures G.4a and b illustrate the "short" waves propagating along the longitudinal axis of a long building or a multiple-span bridge. For simplicity, the incident wave motion has been separated into out-of-plane motion (Fig. G.4-top), consisting of SH and Love waves, and in-plane motion (Fig. G.4-bottom) consisting of P, SV, and Rayleigh waves. The in-plane motion can further be separated into horizontal (longitudinal), vertical, and rocking

components, while out-of-plane motion consists of horizontal motion in the transverse direction and torsion along the vertical axis. Trifunac and Todorovska (1997) analyzed the effects of the horizontal in-plane components of differential motion for buildings with models that are analogous to the sketch in Fig. G.4(bottom), and they showed how the response spectrum method can be modified to include the first-order effects of differential motions. Trifunac and Gicev (2006) showed how to modify the spectra of translational motions, into a spectrum which approximates the total (translational and torsional) responses, and how this approximation is valid for strong motion waves an order of magnitude longer than the structure ($\lambda >> L$).

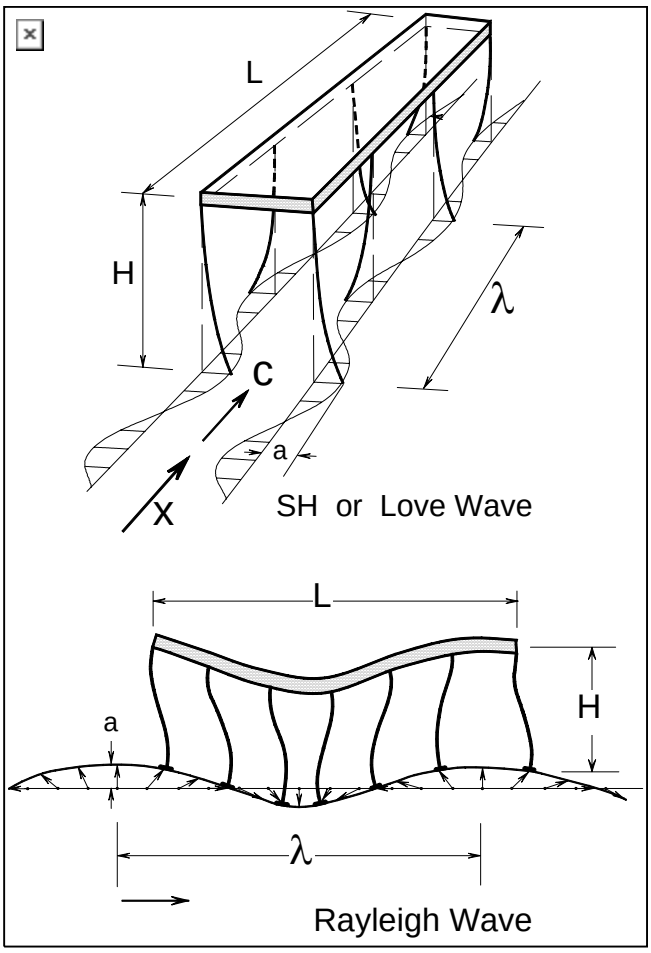

Fig. G.4 Differential out-of-plane response of a long structure excited by SH or Love waves (top), and in-plane response during the passage of Rayleigh waves (bottom).

As can be seen from the above examples the differential motions lead to complex excitation and deformation of the structural members (columns, shear walls, beams, braces), increase the dimensions of the governing differential equations, lead to thee-dimensional dynamic instability problems, and can lead to non-linear boundary conditions. These are all conditions that create environment in which even with the most detailed numerical simulations it is difficult to predict all complexities of the possible responses.

Nonlinear Vibrational Analyses of Response

For estimation of the maximum nonlinear response of a SDOF system, u_m, in terms of the maximum linear response, u_0, it is necessary to specify a relation between u_m and u_0 (Fig. G.5). By defining the yield-strength reduction factor as $R_y = u_0 / u_y$, where u_y is the yielding displacement of the SDOF system equivalent spring, and ductility as $\mu = u_m / u_y$, for the same ground motion, the ratio u_m / u_0 is then equal to μ / R_y. Veletsos and

Newmark (1960) showed that (1) for a long-period SDOF system when its natural period $T_n = 2\pi/\omega_n$ becomes very long, u_m/u_0 tends to 1, and R_y approaches μ (equal deformation rule); (2) for the response amplitudes governed mainly by the peak excitation velocities, u_m/u_0 can be approximated by $\mu/\sqrt{2\mu-1}$ and R_y by $\sqrt{2\mu-1}$ (equal strain energy rule); and (3) for a high-frequency (stiff) system when $T_n \sim 0$, $R_y \sim 1$.

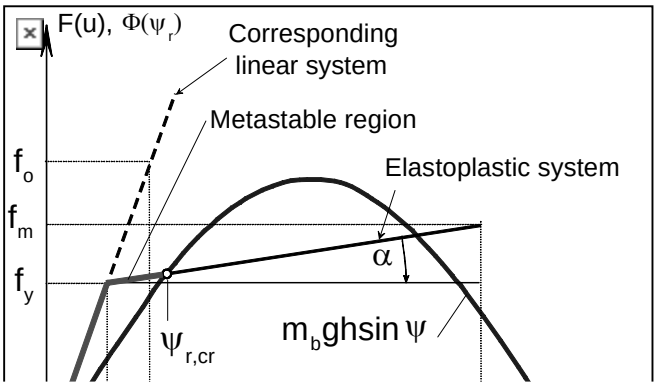

Fig. G.5 Force-displacement (moment-rotation) relationship for bi-linear spring.

Complexities of simultaneous action of dynamic instability, nonlinearity, and kinematic boundary conditions- example. The model we illustrate next is a SDOF, when it is excited by synchronous horizontal ground motion at its two supports (1 and 2), but behaves like a three-degree-of-freedom (3DOF) system, when excited by propagating horizontal, vertical, and rocking ground motions. For such a sytem the classical equal energy and equal displacement rules for SDOF system will not apply.

The purpose here is to describe the effects of differential motion on strength-reduction factors of the simple structure shown in Figure G.6, when it is subjected to all components of near-source ground motions and to illustrate the resulting complexities of nonlinear response. Analyses of the consequences of the differences in ground motion at structural supports, caused by non-uniform soil properties, soil-structure interaction, and lateral spreading, for example, will further contribute to the complexities of the response, but will not be discussed here.

The original response spectrum method has been formulated using a vibrational solution of the differential equation of a SDOF system, excited by synchronous, and only horizontal (one component) representation of ground motion. The role of simultaneous action of all six components of ground motion (three translations and three rotations) is still rarely considered in modern engineering design (Trifunac 2006), even though it has been 75 years since the response spectrum method was formulated and about 40 years since it became the principal tool in engineering design (Trifunac 2003). Because the response spectrum method has become an essential part of engineering design and of the description process of how future strong motion should be specified for a broad range of design applications (Todorovska et al. 1995), we hope that the present examples will help to further understand the complexities of response in more realistic models of structures.

The nature of relative motion of individual column foundations or of the entire foundation system will depend upon the type of foundation, the characteristics of the soil surrounding the foundation, the type of incident waves, and the direction of wave arrival, such that at the base of each column the motion has six degrees of freedom. In this example we assume that the effects of soil-sructure interaction are negligible, consider only the in-plane horizontal, vertical, and rocking components of motion of column foundations, and show selected results of the analysis for structures on isolated foundations only. We assume that the structure is near the fault and that the longitudinal

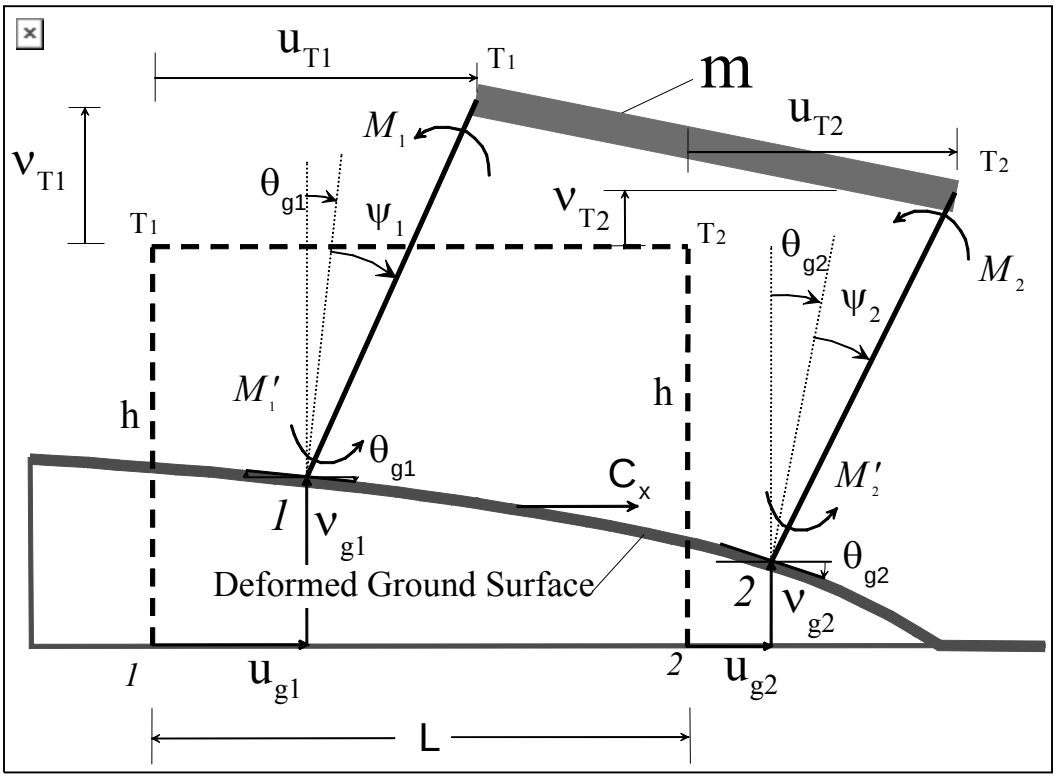

Fig. G.6 The system deformed by the wave, propagating from left to right, with phase velocity C_x, for the case of $+v_{oi}$ ("up" motion).

axis of the structure (X axis) coincides with the radial direction (r axis) of the propagation of waves from the earthquake source so that the displacements at the base of columns are different as a result of the wave passage only. We suppose that the excitations at piers have the same amplitude with different phases. The phase difference (or time delay) will depend upon the distance between piers and the horizontal phase velocity of the incident waves.

The simple model we consider is described in Fig. G.6. It represents a one-story structure consisting of a rigid mass, *m,* with length *L,* supported by two rigid mass-less columns with height *h*, which are connected at the top to the mass and at the bottom to the ground by rotational springs (not shown in Fig.G.6). The stiffness of the springs, k_ϕ, is assumed

to be elastic-plastic, as in Fig. G.5, without hardening ($\alpha = 0$). The mass-less columns are connected to the ground and to the rigid mass by rotational dashpots, c_ϕ, providing a fraction of critical damping equal to 5 percent. Rotation of the columns, $\phi_i = \theta_{gi} + \psi_i$ for i=1,2, which is assumed not to be small, leads us to consider the geometric nonlinearity. The mass is acted upon by the acceleration of gravity, g, and is excited by differential horizontal, vertical, and rocking ground motions, u_{g_i}, v_{g_i}, and $\theta_{g_i}, i = 1,2$ (Fig. G.6) at two bases so that

$u_{g_2}(t) = u_{g_1}(t-\tau)$; $v_{g_2}(t) = v_{g_1}(t-\tau)$; $\theta_{g_2}(t) = \theta_{g_1}(t-\tau)$; $\tau = L/C_x$,

with τ being the time delay between motions at the two piers and C_x the horizontal phase velocity of incident waves. The functional forms of u_{g_i}, v_{g_i}, and θ_{g_i} are defined by near-source ground motions (Jalali and Trifunac 2007). The rocking component of the ground motion will be approximated by (Lee and Trifunac 1987) $\theta_{g_i}(t) = -\dot{v}_{g_i}(t)/C_x$, where $\dot{v}_{g_i}(t)$ is the vertical velocity of the ground motion at the *i-th* column. Of course, in a more accurate modeling, the ratio of v_{g_i} to u_{g_i} amplitudes will depend on the incident angle and the character of incident waves, while the associated rocking θ_{g_i} will be described by a superposition of rocking angles associated with incident body and dispersed surface waves (Lee and Trifunac 1987).

The yield-strength reduction factor for the system subjected to synchronous ground motion is $R_y = f_0 / f_y = u_0 / u_y$, where all of the quantities are defined in Fig. G.5. In this work, for the assumed model and because of differential ground motions and rotation of the beam, the relative rotation for two columns at their top and bottom will be different. Therefore, it is necessary to define the *R*-factor and ductility for each corner of the system, instead of one factor for the total system. In all calculations here we consider the actions of the horizontal, vertical, and rocking components of the ground motion, the effects of gravity force, dynamic instability, and geometric non-linearity. For the structure in Fig. G.6, we calculate maximum linear and nonlinear relative rotations at four corners of the system under downward $(-v_{g_i})$, radial, and rocking, and upward $(+v_{g_i})$, radial, and rocking near-source differential ground motions corresponding to given earthquake magnitude, ductility μ, and for a time delays, τ. Then we plot R_y versus T_n for four corners of the system. Iterations are required to compute the inelastic deformation ratio for a specified ductility factor because different values of moments may lead to the same ductility. The convention is to choose the largest moment (Veletsos and Newmark 1964).

Fig. G.7 illustrates typical results for R_y versus the oscillator period for near-source, fault-parallel displacement, $d_N(t) = A_N(1 - e^{-t/\tau_N})/2$ (Jalali and Trifunac 2007), with downward vertical ground displacement, magnitude *M* = 8, for ductility ratio of eight, and time delay $\tau = 0.05$ s. It shows the results for the top-left, top-right, bottom-left, and bottom-right corners of the system, assuming wave propagation from left to right (see Fig. G.6). For reference and easier comparison with the previously published results, we

also plot one of the oldest estimates of R_y versus period, using piecewise straight lines (Jalali and Trifunac 2007). The curve $(R_y)_{\min}$ shows the minimum values of R_y for $d_N(t)$ motion with $-v_{g_i}$, and for M = 8, $\mu = 8$, and $\tau = 0.05$ s.

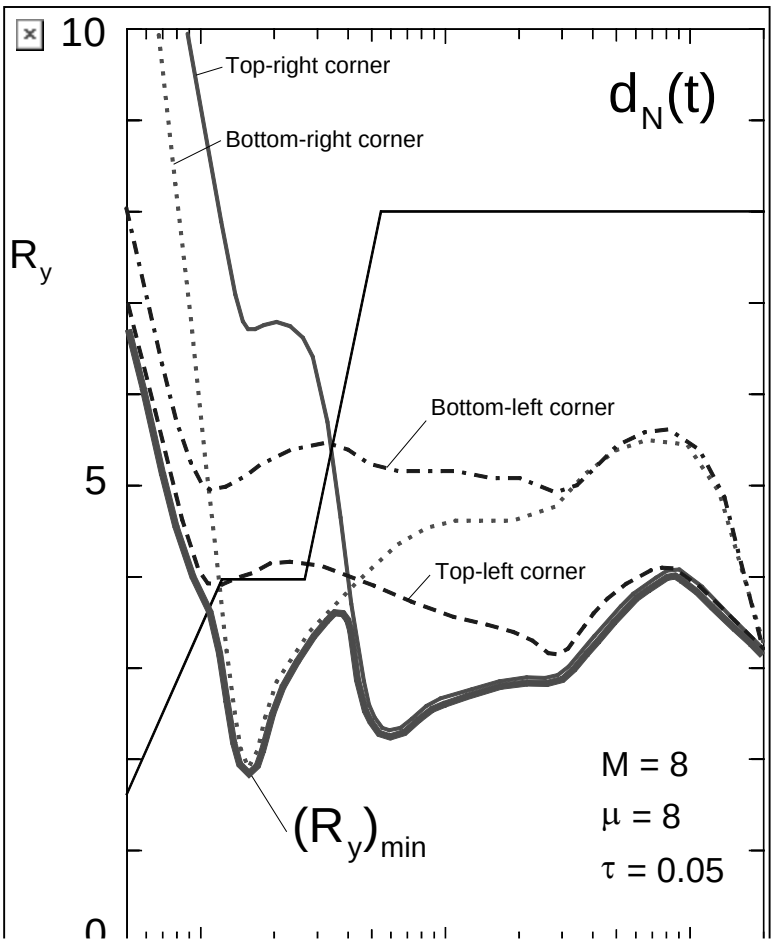

Fig. G.7 R_y versus oscillator period for near-source, fault-parallel displacement, downward vertical ground displacement, magnitude M = 8, for ductility ratio of eight, and time delay $\tau = 0.05$ s. The oldest estimates of R_y versus period are shown using piecewise straight lines (Jalali et al. 2007). For this set of parameters the curve $(R_y)_{\min}$ shows the minimum values of R_y versus period.

For periods longer than 5 to 10 s, R_y curves approach "collapse boundaries" (Jalali and Trifunac 2007). This is implied in Fig. G.7 by rapid decrease of R_y versus period, for periods longer than about seven seconds. At or beyond these boundaries, the nonlinear system collapses due to action of gravity loads and dynamic instability.

The complex results illustrated in Fig. G.7 can be simplified by keeping only $(R_y)_{\min}$, since it is only the minimum value of R_y that is needed for engineering design. By mapping $(R_y)_{\min}$ versus period of the oscillator, for different earthquake magnitudes, M, different ductilities, μ, and different delay times τ, design criteria can be formulated for design of simple structures to withstand near-fault differential ground motions (Jalali and Trifunac 2007). Nevertheless the above

shows how complicated the response becomes even for as simple structure as the one shown by the model in Fig. G.6, when differential ground motion with all components of motion is considered. In this example this complexity results from simultaneous consideration of material and geometric nonlinearities, dynamic instability, and kinematic boundary conditions.

References

Biot, M.A. (2006). Influence of Foundation on Motion of Blocks, *Soil Dynamics & Earthquake Engrg*, 26(6–7), 486–490.

Bycroft, G. N. (1980). Soil-Foundation Interaction and Differential Ground Motions, *Earthquake Engineering and Structural Dynamics*, 8(5), 397-404.

Gicev, V. (2005). Investigation of soil-flexible foundation-structure interaction for incident plane SH waves, *Ph.D. Dissertation*, Dept. of Civil Engineering, Univ. Southern California, Los Angeles, California.

Gicev, V. and Tifunac, M.D. (2006a). Rotations in the Transient Response of Nonlinear Shear Beam, *Dept. of Civil Engineering Report* CE 06-02, Univ. Southern California, Los Angeles, California.

Jalali, R., and Trifunac, M.D. (2007). Strength-Reduction Factors for Structures Subjected to Differential Near-Source Ground Motion, *Indian Society of Earthquake Technology Journal* , 44(1), (in Press).

Lee, V.W. (1979). Investigation of Three-Dimensional Soil-Structure Interaction, *Department of Civil Engineering,* Report CE. 79-11, Univ. of Southern California, Los Angeles, California.

Lee, V.W., and Trifunac, M.D. (1982). Body Wave Excitation of Embedded Hemisphere, *ASCE, EMD*, 108(3), 546–563.

Lee, V.W., and Trifunac, M.D. (1985). Torsional Accelerograms, *Int. J. Soil Dynamics and Earthquake Engineering*, 4(3), 132-139.

Lee, V.W., and Trifunac, M.D. (1987). Rocking Strong Earthquake Accelerations, *Int. J. Soil Dynamics and Earthquake Eng*., 6(2), 75-89.

Todorovska. M. I., & Trifunac, M. D. (1990). Note on excitation of long structures by ground waves. *ASCE, EMD*, 116(4), 952-964, and Errata in 116, 1671.

Trifunac, M.D. (2003). 7*0-th Anniversary of Biot Spectrum, 23-rd Annual ISET Lecture,* Indian Society of Earthquake Technology, Vol. 40, No. 1, 19-50.

Trifunac, M.D. (2006). Effects of Torsional and Rocking Excitations on the Response of Structures, Ch. 42 in *Earthquake Source Asymmetry, Structural Media and Rotation Effects*, R. Teisseyre, M. Takeo, and E. Majewski (eds.), Springer, Heidelberg, Germany.

Trifunac, M.D., and Gicev,V. (2006). Response Spectra for Differential Motion of Columns, Paper II: Out-of-Plane Response, *Soil Dynamics and Earthquake Engineering*, **26**(12), 1149-1160.

Trifunac, M.D. and Novikova, E.I., (1994). State of the Art Review on Strong Motion Duration, *10th European Conf. on Earthquake Eng*., Vol. I,131-140.

Trifunac, M. D., & Todorovska, M.I. (1997). Response Spectra and Differential Motion of Columns. *Earthquake Eng. and Structural Dyn.*, 26(2), 251-268.

Trifunac, M.D., Ivanovic, S.S., and Todorovska, M.I. (2001a). Apparent Periods of a Building I: Fourier Analysis, *J. of Struct. Engrg*, ASCE, 127(5), 517–526.

Trifunac, M.D., Ivanovic, S.S., and Todorovska, M.I. (2001b). Apparent Periods of a Building II: Time-Frequency Analysis, *J. of Struct. Engrg*, ASCE, 127(5), 527–537.

Trifunac, M.D., Hao, T.Y., and Todorovska, M.I. (2001c). Response of a 14-Story Reinforced Concrete Structure to Nine Earthquakes: 61 Years of Observation in the Hollywood Storage Building, *Dept. of Civil Engrg., Report* CE 01-02, Univ. of Southern California, Los Angeles, California.

Veletsos, A.S., and Newmark, N.M. (1964). *Response Spectra for Single-Degree-of-Freedom Elastic and Inelastic Systems*, Rep. No. RTD-TDR-63-3096, Vol. III, Air Force Weapons Lab., Albuquerque, N. M.

Wong, H.L., and Trifunac, M.D. (1979). Generation of Artificial Strong Motion Accelerograms, *Int. J. Earthquake Engineering Struct. Dynamics*, 7(6), 509-527.